Types of foliations

- **Crenulation Cleavage-**
  - Actually consists of 2 cleavages
  - The first may be a *slaty cleavage* or *schistosity* that becomes *microfolded*
  - Fold axial planes typically form at high angle to the σ_1 of the second compressional phase

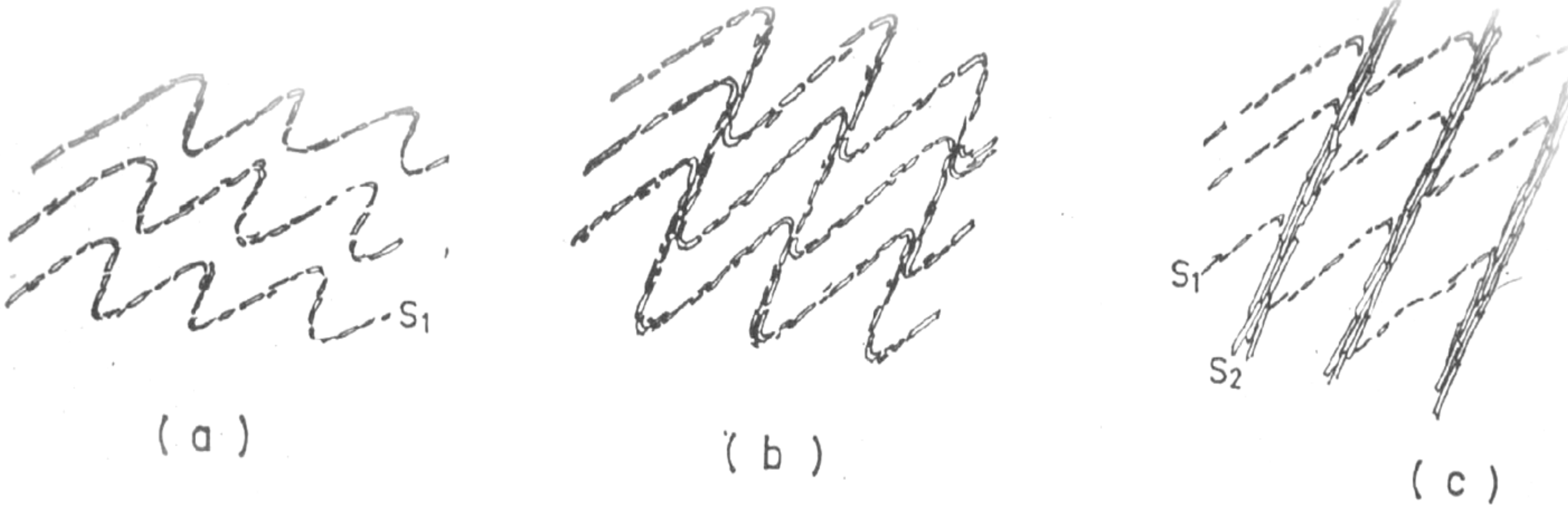

Progressive development (a → c) of a crenulation cleavage for both asymmetric (top) and symmetric (bottom) situations. From Spry (1969) *Metamorphic Textures*. Pergamon. Oxford.

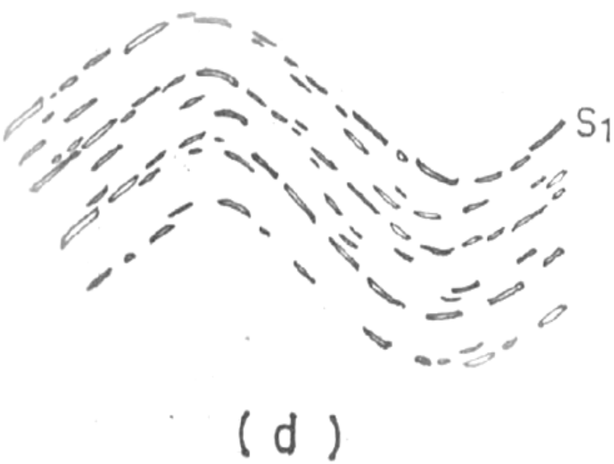

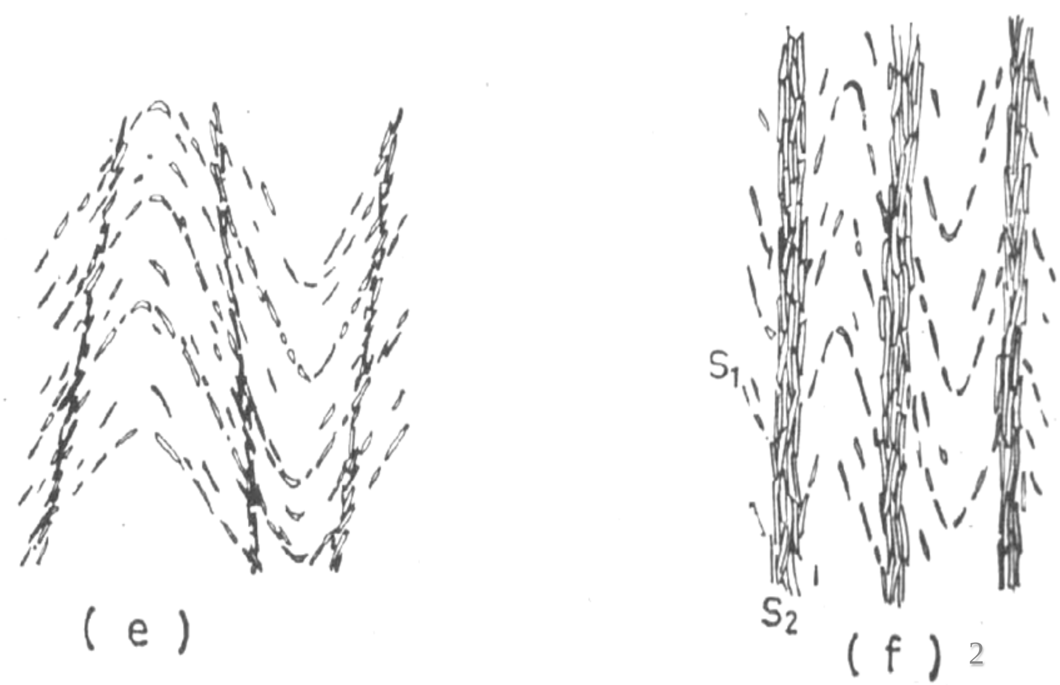

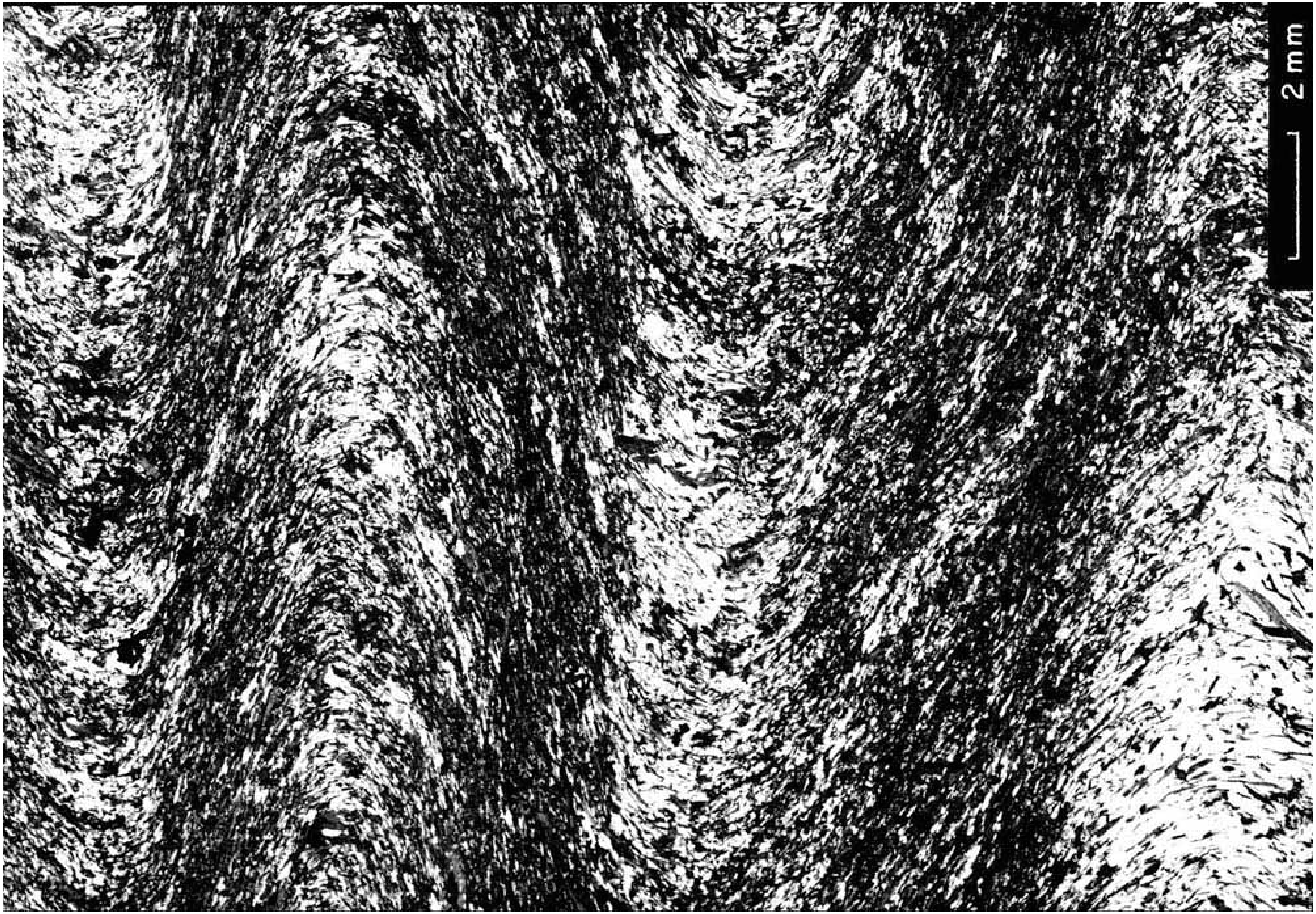

Figure 23.24a. Symmetrical crenulation cleavages in amphibole-quartz-rich schist. Note concentration of quartz in hinge areas. From Borradaile *et al*. (1982) *Atlas of Deformational and Metamorphic Rock Fabrics*. Springer-Verlag.

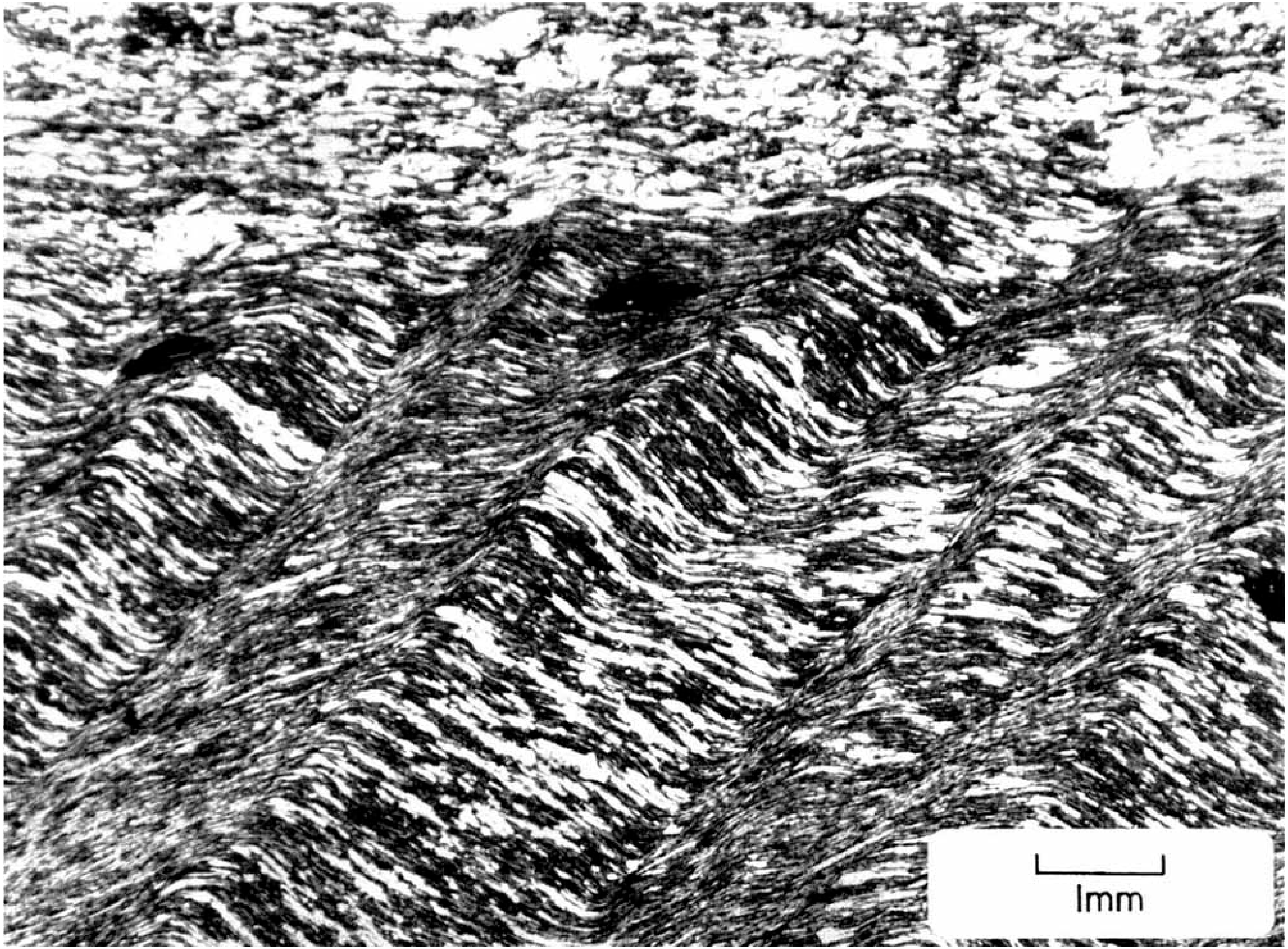

Figure 23.24b. Asymmetric crenulation cleavages in mica-quartz-rich schist. Note horizontal compositional layering (relict bedding) and preferential dissolution of quartz from one limb of the folds. From Borradaile *et al*. (1982) *Atlas of Deformational and Metamorphic Rock Fabrics*. Springer-Verlag.

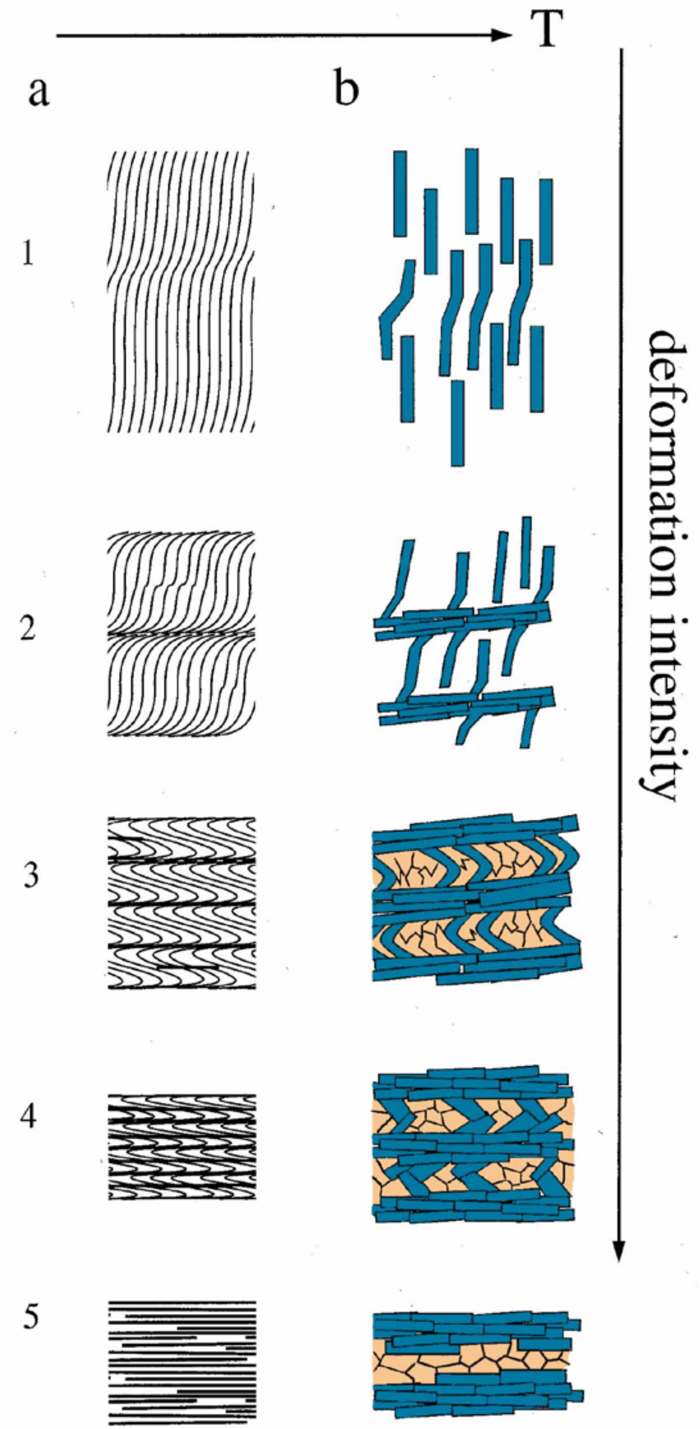

Figure 23.25. **Stages in the development of crenulation cleavage as a function of temperature and intensity of the second deformation. From Passchier and Trouw (1996) *Microtectonics*. Springer-Verlag.**

Development of S_2 micas depends upon T and the intensity of the second deformation

Types of lineations

a. Preferred orientation of elongated mineral aggregates

b. Preferred orientation of elongate minerals

c. Lineation defined by platy minerals

d. Fold axes (especially of crenulations)

e. Intersecting planar elements.

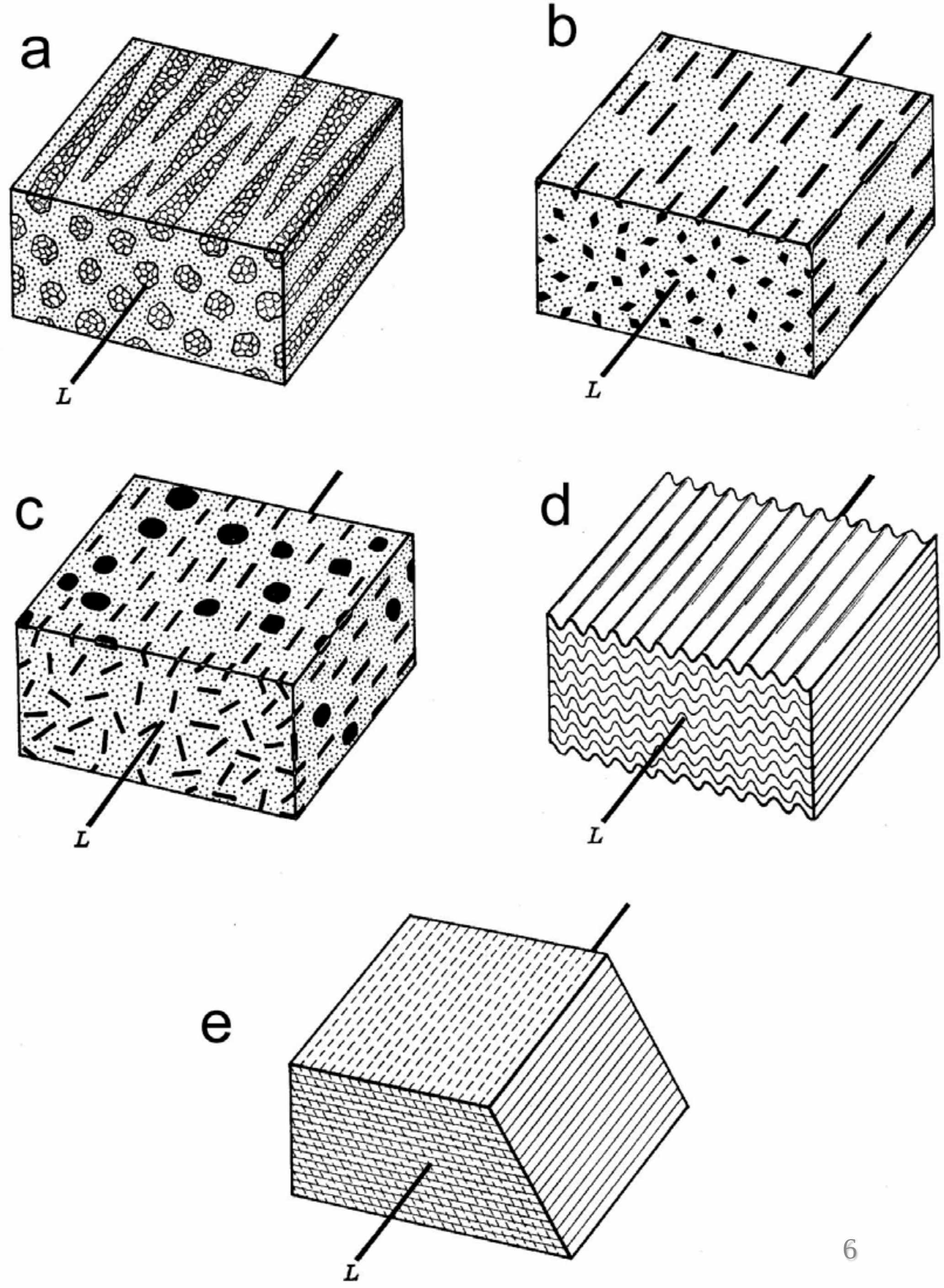

Figure 23.26. Types of fabric elements that define a lineation. From Turner and Weiss (1963) *Structural Analysis of Metamorphic Tectonites.* McGraw Hill.

Analysis of Deformed Rocks

- If two or more geometric elements are present, we can add a numeric subscript to denote the chronological sequence in which they were developed and superimposed-

- Deformational events: D_1 D_2 D_3 …
- Metamorphic events: M_1 M_2 M_3 …
- Foliations: S_o S_1 S_2 S_3 …
- Lineations: L_o L_1 L_2 L_3 …
- Plot on a metamorphism-deformation-time plot showing the crystallization of each mineral

Deformation vs. Metamorphic Mineral Growth

Deformation vs. Metamorphic Mineral Growth

- **Pre-kinematic** – crystals that show the usual characteristics of minerals affected by later deformation – these include:
  - Undulose extinction
  - Cracked and broken crystals
  - Deformation bands
  - Twins
  - Kink bands
  - Pressure shadows
  - Porphyroclasts with mortar texture or sheared rims (mantles)

Pre-kinematic crystals

a. Bent crystal with undulose extinction
b. Foliation wrapped around a porphyroblast
c. Pressure shadow or fringe
d. Kink bands or folds
e. Microboudinage
f. Deformation twins

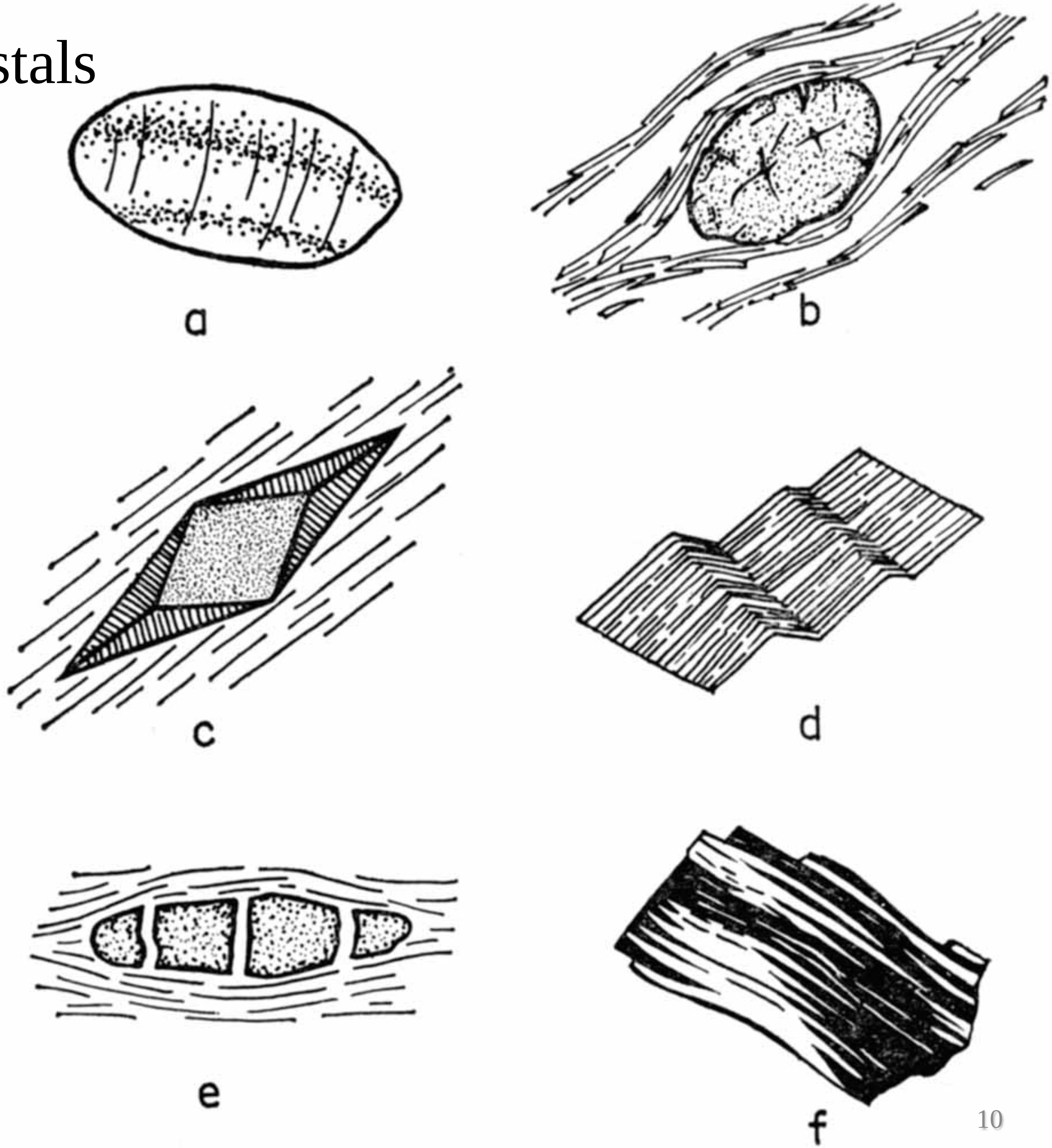

Figure 23.34. **Typical textures of pre-kinematic crystals. From Spry (1969) *Metamorphic Textures*. Pergamon. Oxford.**

Deformation vs. Metamorphic Mineral Growth

- **Post-kinematic** – crystallization either outlasted deformation or occurred in a distinct later thermal or contact event. This results in:
  - Unstrained, randomly oriented crystals and cut across an earlier foliation (next slide 23.35b)
  - **Pseudomorphs** (next slide 23.35f) – a precursor crystal is replaced by an aggregate of random smaller crystals
  - **Polygonal arcs** (next slide 23.35c) – folded, elongate minerals polygonize to an arcuate pattern consisting of smaller straight crystals

Post-kinematic crystals

a. Helicitic folds **b.** Randomly oriented crystals **c.** Polygonal arcs
d. Chiastolite **e.** Late, inclusion-free rim on a poikiloblast (?)
f. Random aggregate pseudomorph

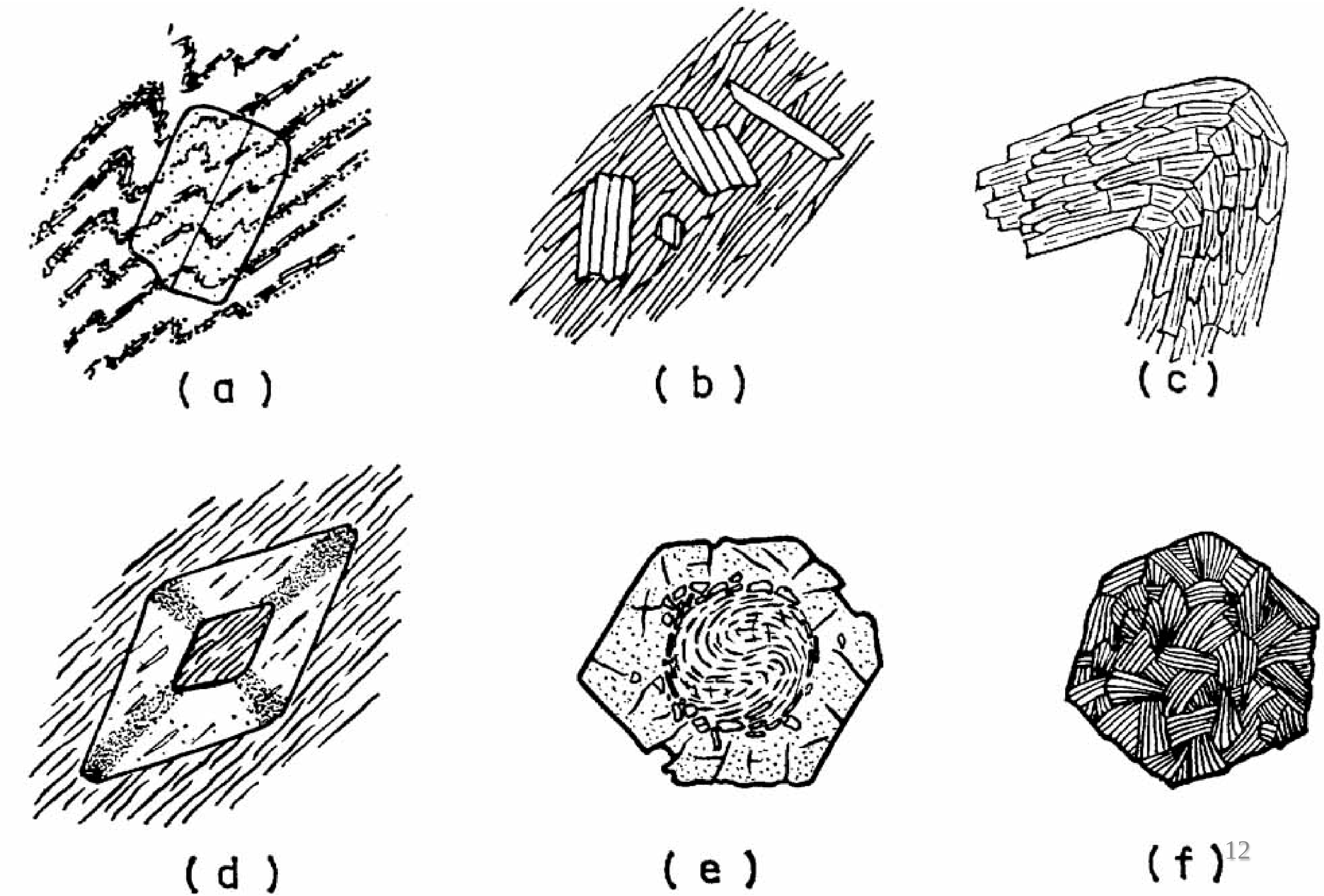

Figure 23.35. **Typical textures of post-kinematic crystals. From Spry (1969) *Metamorphic Textures*. Pergamon. Oxford.**

Deformation vs. Metamorphic Mineral Growth

- **Syn-kinematic** – mineral growth is probably the most common type in ***orogenic metamorphism*** since metamorphism and deformation are believed to go “hand in hand”

Syn-kinematic crystals

Paracrystalline microboudinage

Spiral Porphyroblast

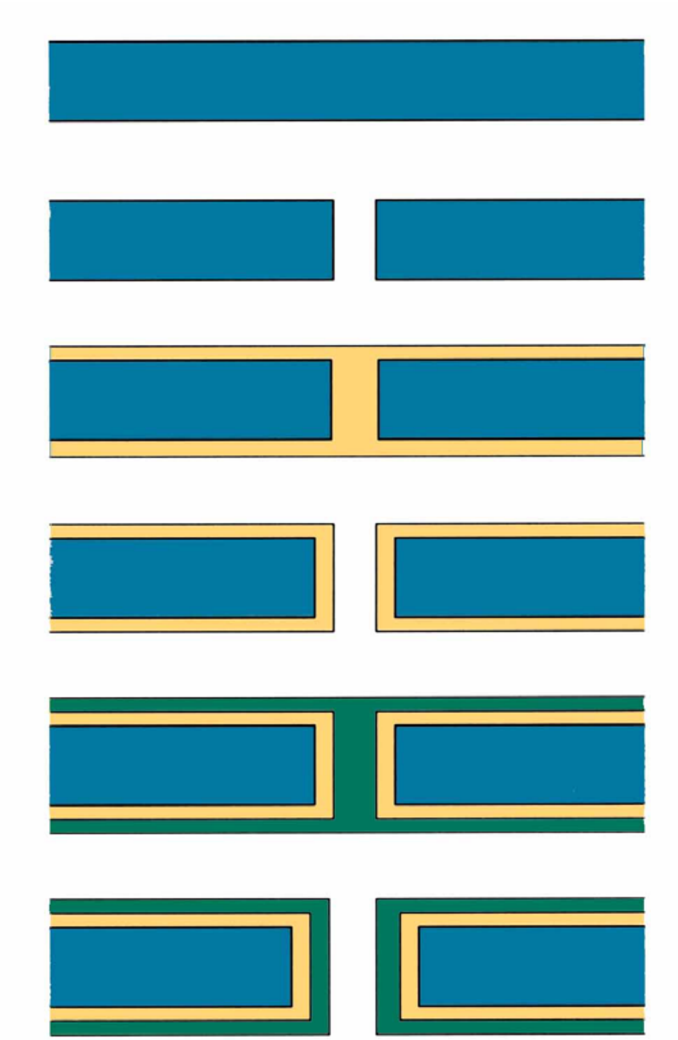

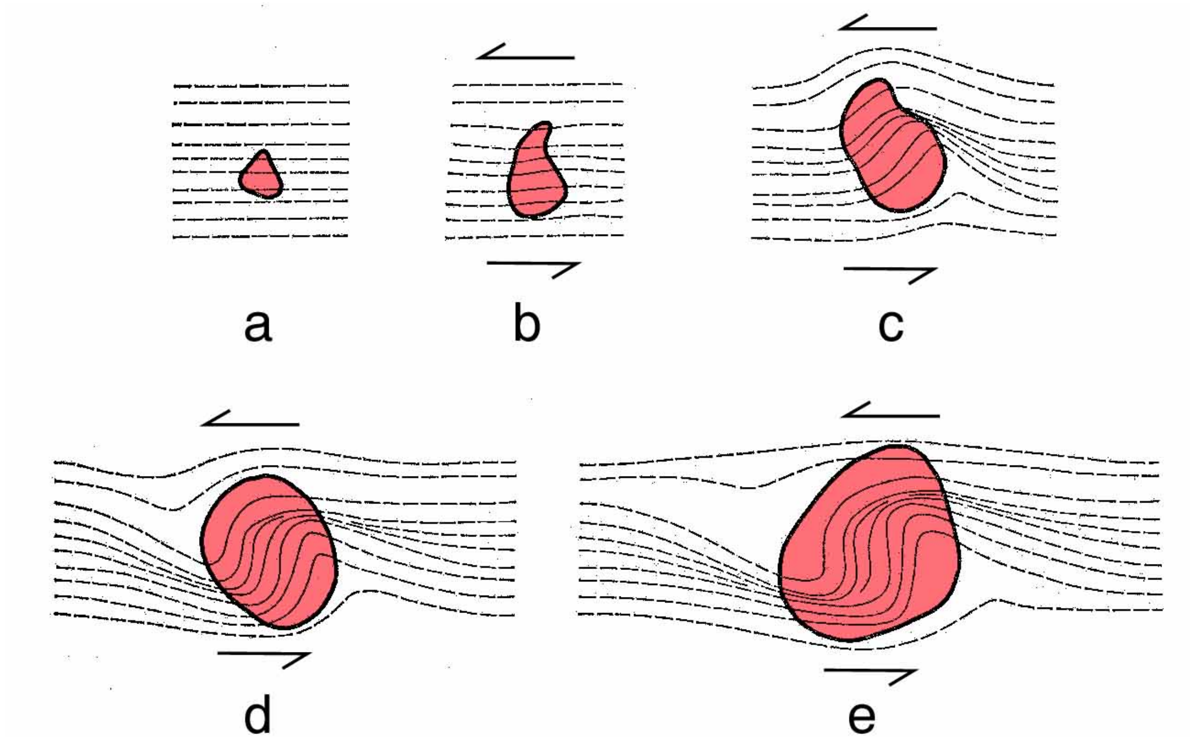

Figure 23.38. Traditional interpretation of spiral S_i train in which a porphyroblast is rotated by shear as it grows. From Spry (1969) *Metamorphic Textures*. Pergamon. Oxford.

Figure 23.36. Syn-crystallization micro-boudinage. Syn-kinematic crystal growth can be demonstrated by the color zoning that grows and progressively fills the gap between the separating fragments. After Misch (1969) *Amer. J. Sci.*, 267, 43.63.

Syn-kinematic crystals

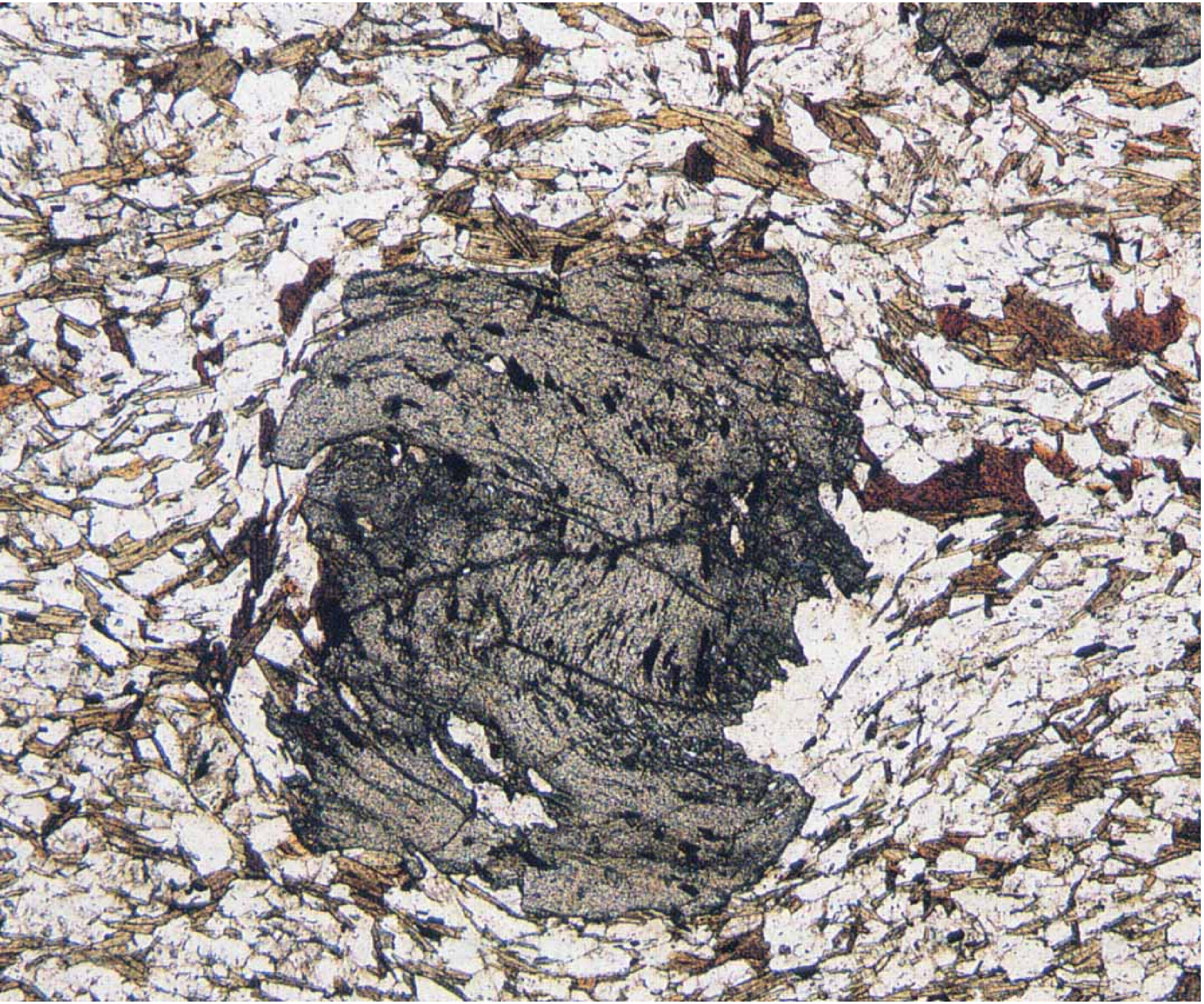

Figure 23.38. **Spiral S_i train in garnet, Connemara, Ireland. Magnification ~20X. From Yardley *et al*. (1990) *Atlas of Metamorphic Rocks and their Textures*. Longmans.**

Syn-kinematic crystals

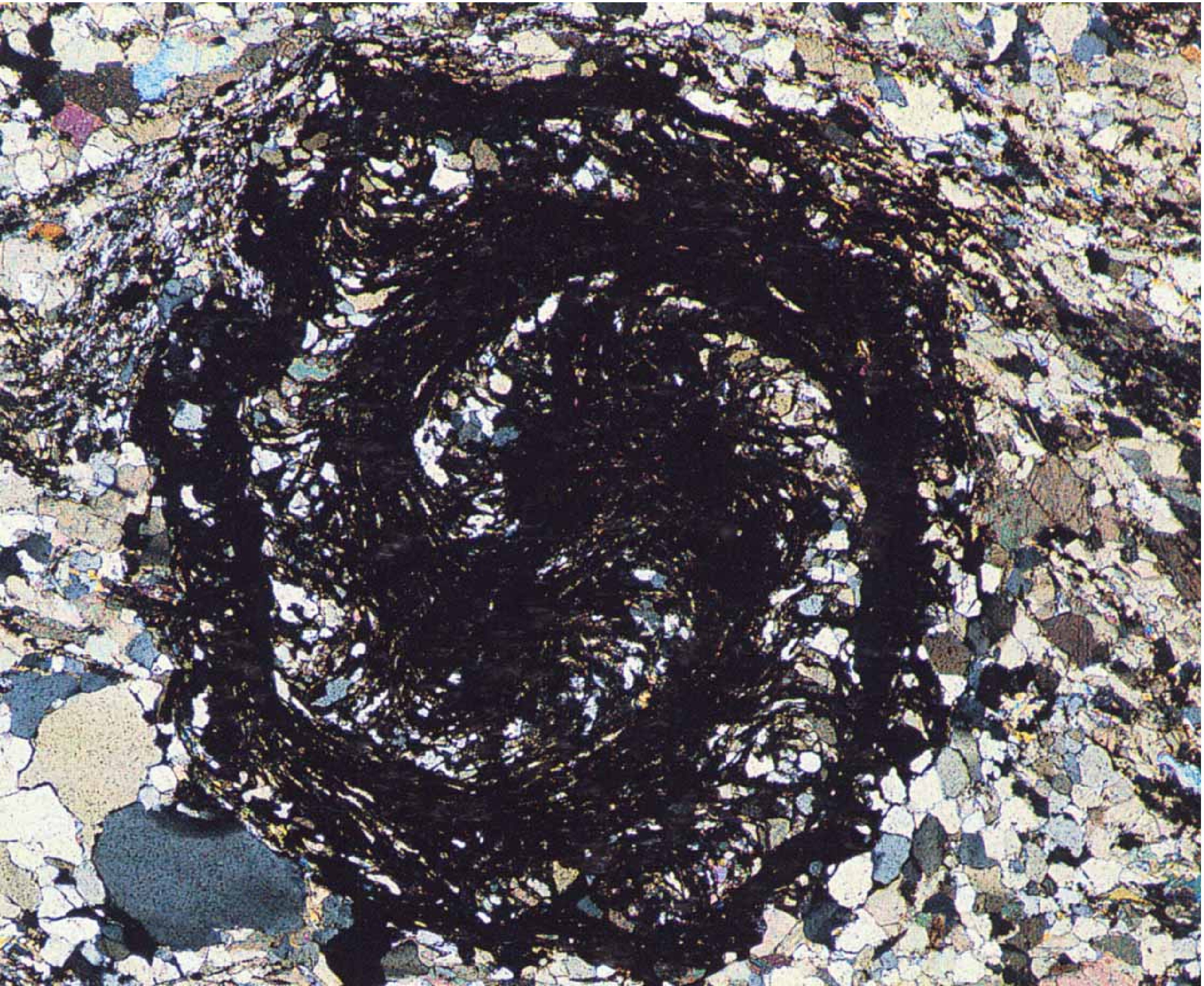

Figure 23.38. **"Snowball garnet" with highly rotated spiral S_i. Porphyroblast is ~ 5 mm in diameter. From Yardley *et al*. (1990) *Atlas of Metamorphic Rocks and their Textures*. Longmans.**

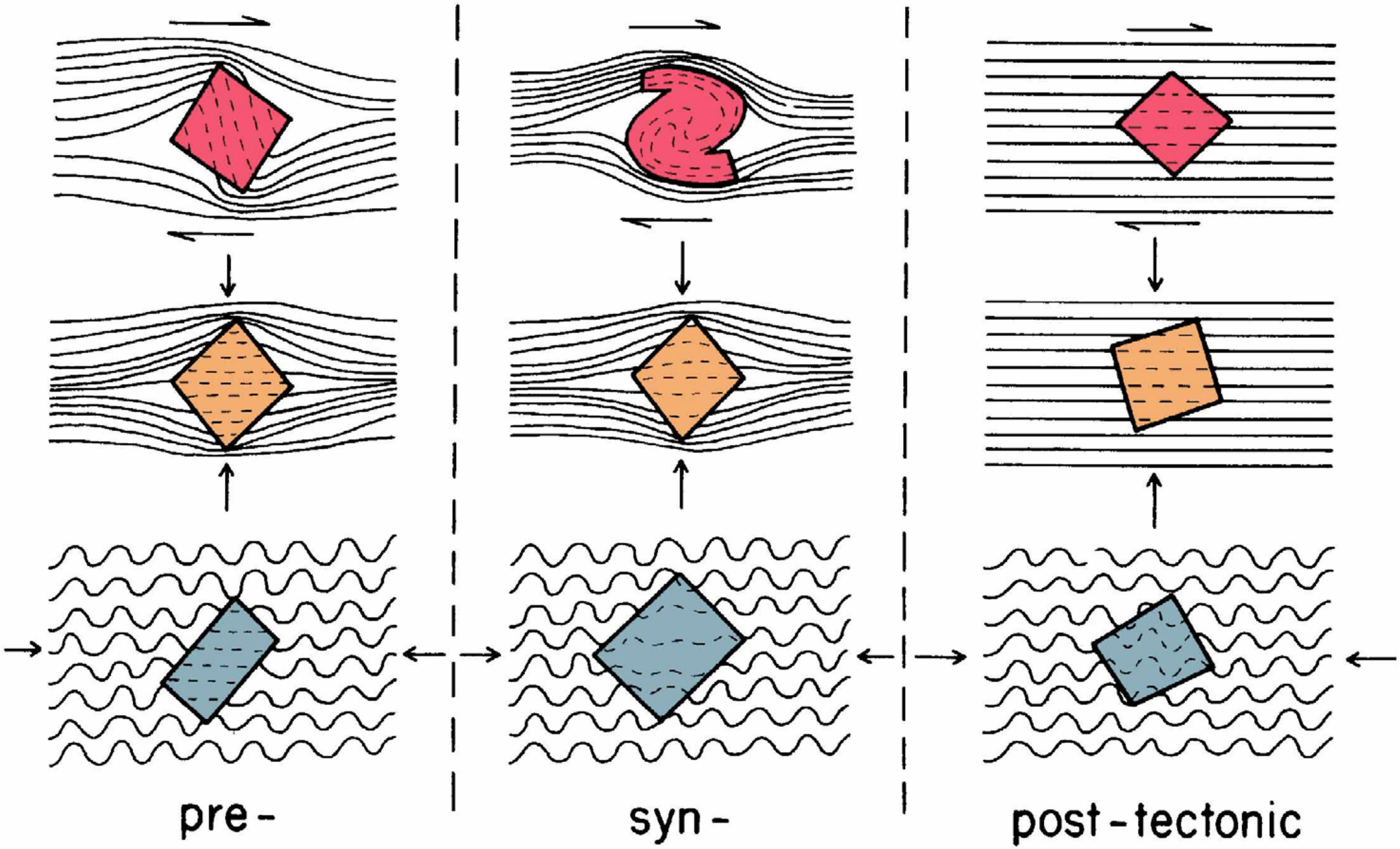

Figure 23.37. S_i **characteristics of clearly pre-, syn-, and post-kinematic crystals as proposed by Zwart (1962). a. Spiraled** S_i **due to rotation of the matrix or the porphyroblast during growth. b. Progressively flattened** S_i **from core to rim. c. Progressively more intense folding of** S_i **from core to rim. c. After Zwart (1962)** ***Geol. Rundschau*****, 52, 38-65.**

Syn-kinematic crystals

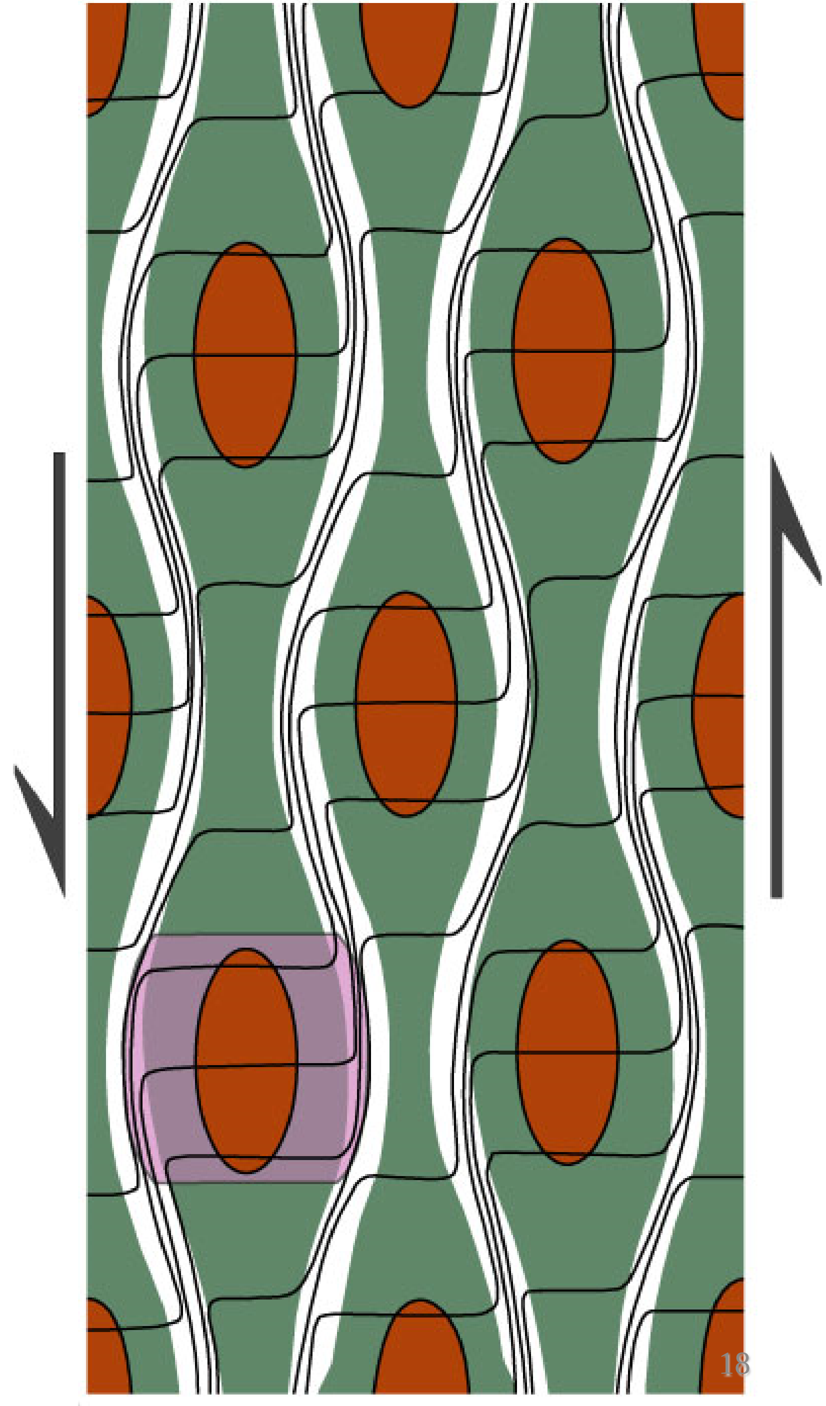

Figure 23.40. **Non-uniform distribution of shear strain as proposed by Bell *et al*. (1986) *J. Metam. Geol.*, 4, 37-67. Blank areas represent high shear strain and colored areas are low-strain. Lines represent initially horizontal inert markers (S_1). Note example of porphyroblast growing preferentially in low-strain regions.**

Analysis of Deformed Rocks

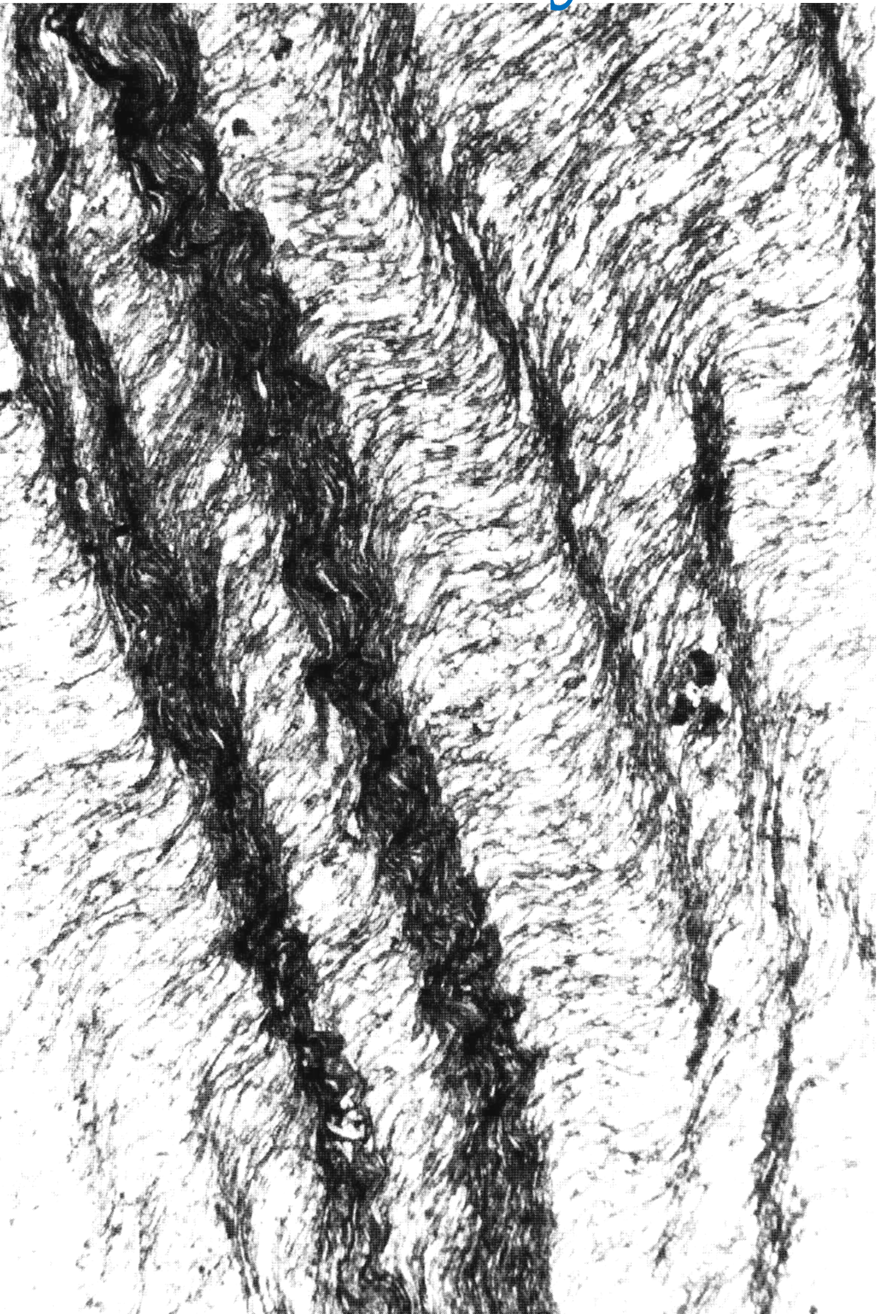

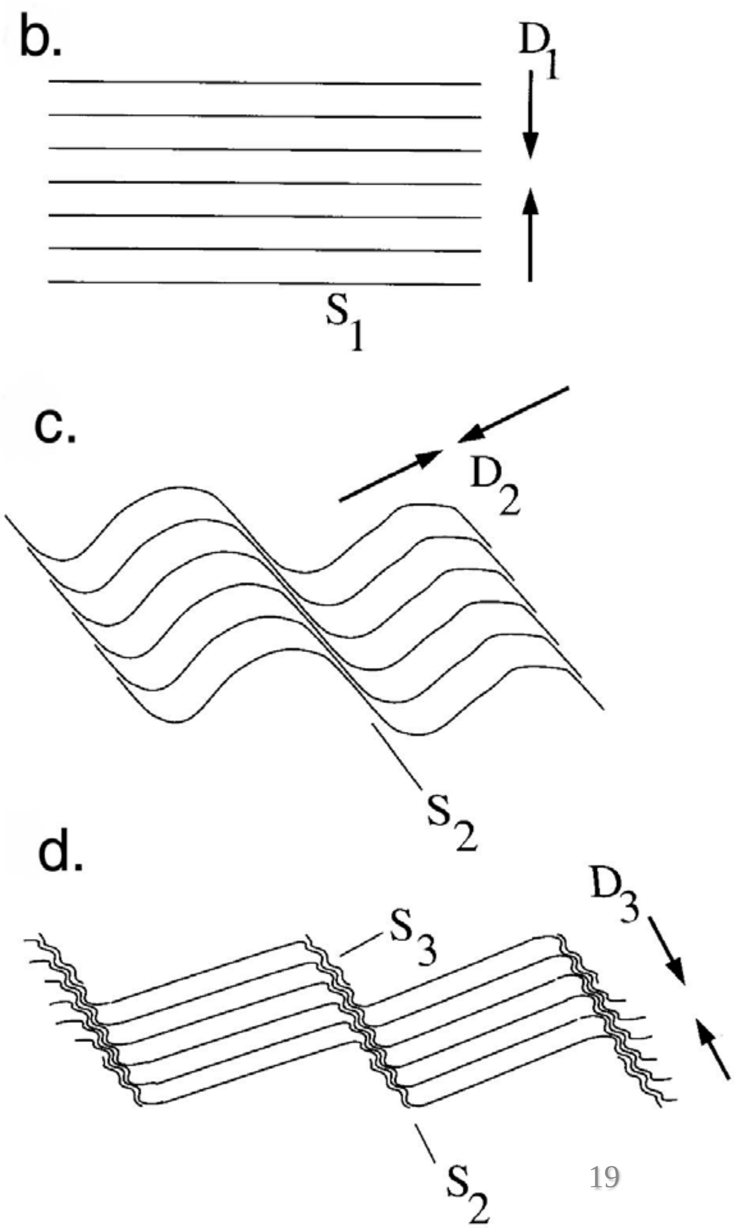

Figure 23.42. **(left) Asymmetric crenulation cleavage (S_2) developed over S_1 cleavage. S_2 is folded, as can be seen in the dark sub-vertical S_2 bands. Field width ~ 2 mm. Right: sequential analysis of the development of the textures. From Passchier and Trouw (1996) Microtectonics. Springer-Verlag.**

Analysis of Deformed Rocks

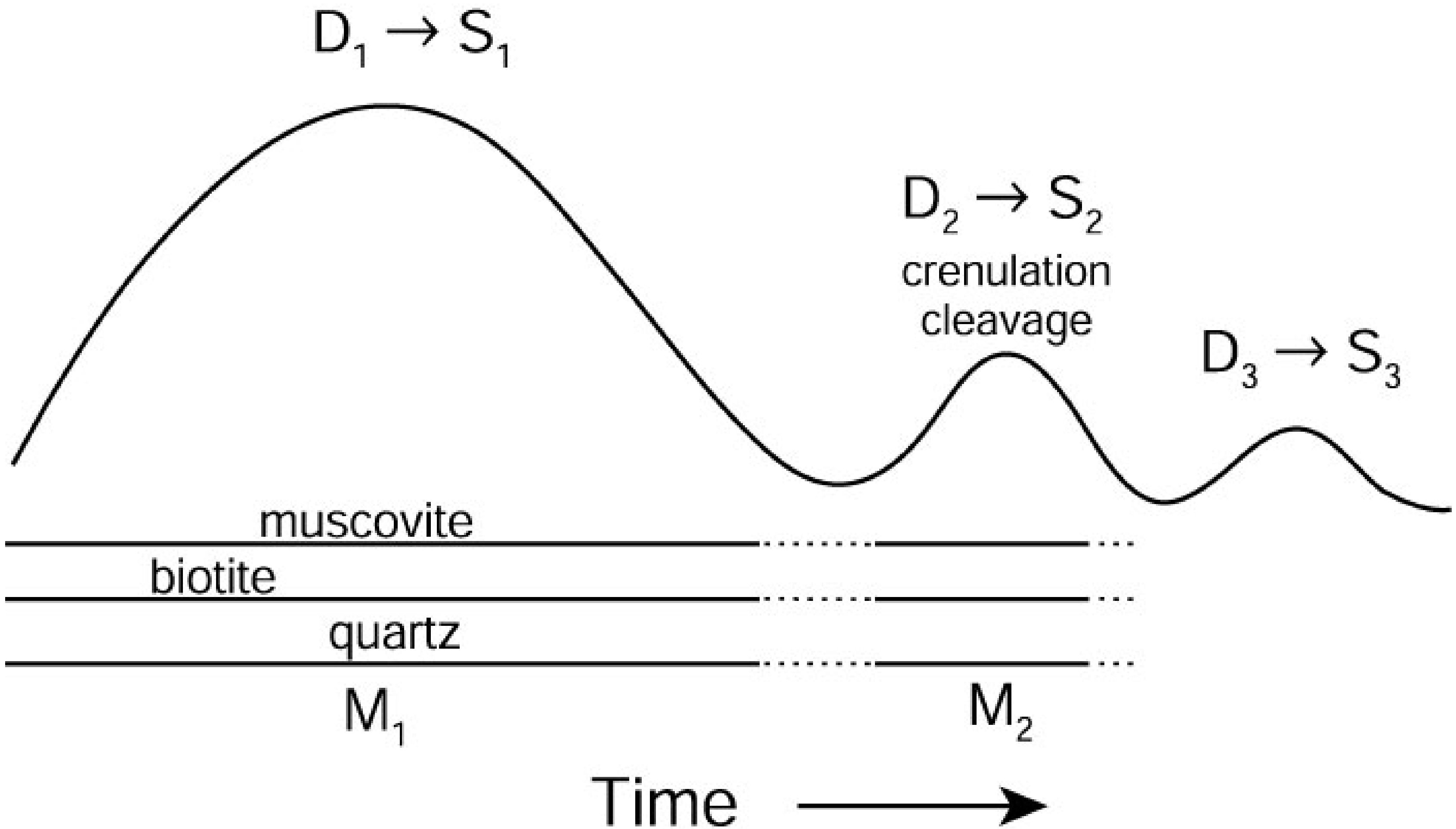

Figure 23.43. **Graphical analysis of the relationships between deformation (D), metamorphism (M), mineral growth, and textures in the rock illustrated in Figure 23.42. Winter (2010) *An Introduction to Igneous and Metamorphic Petrology.* Prentice Hall.**

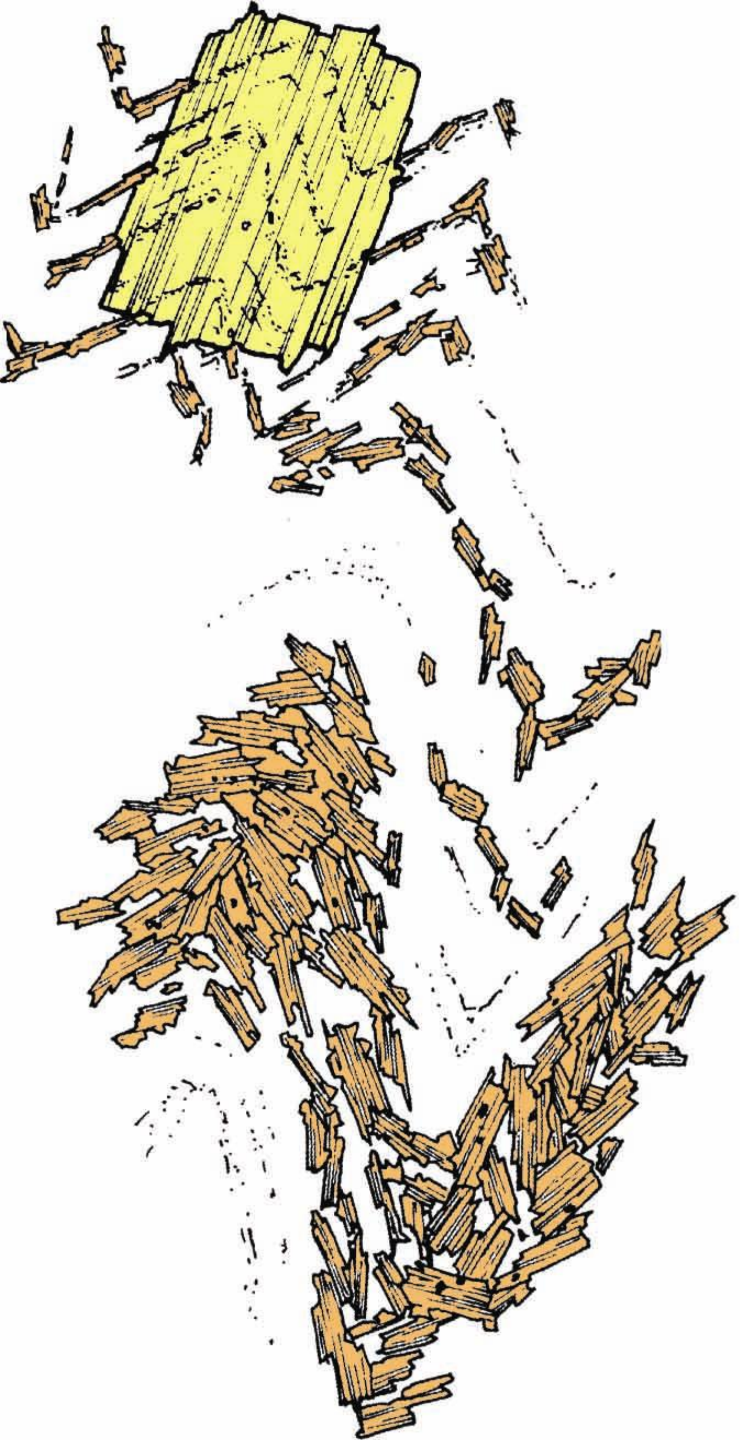

Figure 23.46. **Textures in a hypothetical andalusite porphyryoblast-mica schist. After Bard (1986) *Microtextures of Igneous and Metamorphic Rocks*. Reidel. Dordrecht.**

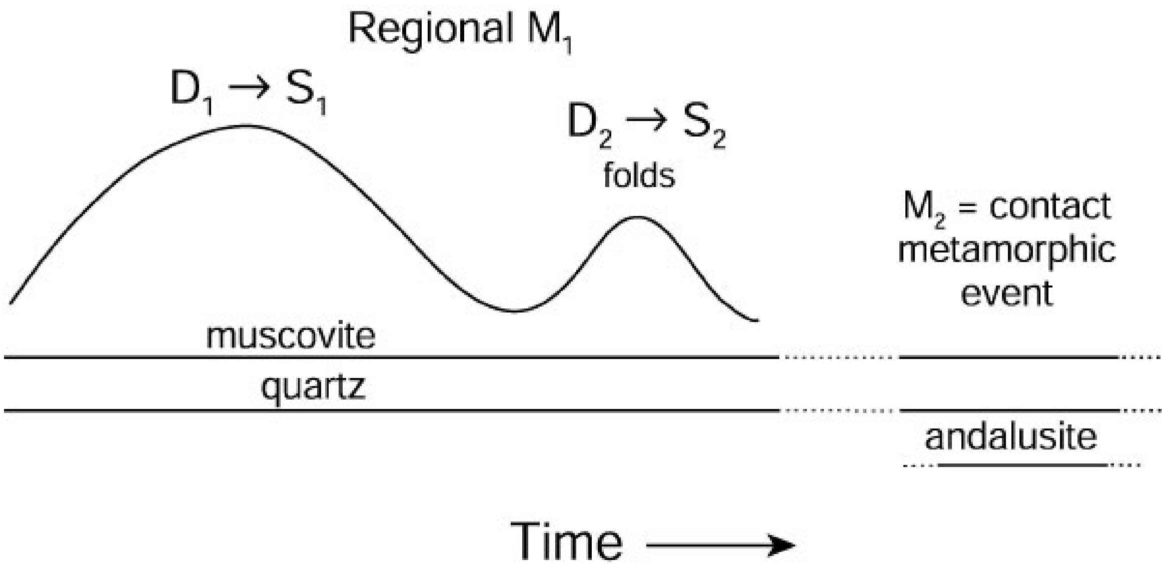

Figure 23.47. **Graphical analysis of the relationships between deformation (D), metamorphism (M), mineral growth, and textures in the rock illustrated in Figure 23.46. Winter (2010) *An Introduction to Igneous and Metamorphic Petrology.* Prentice Hall.**

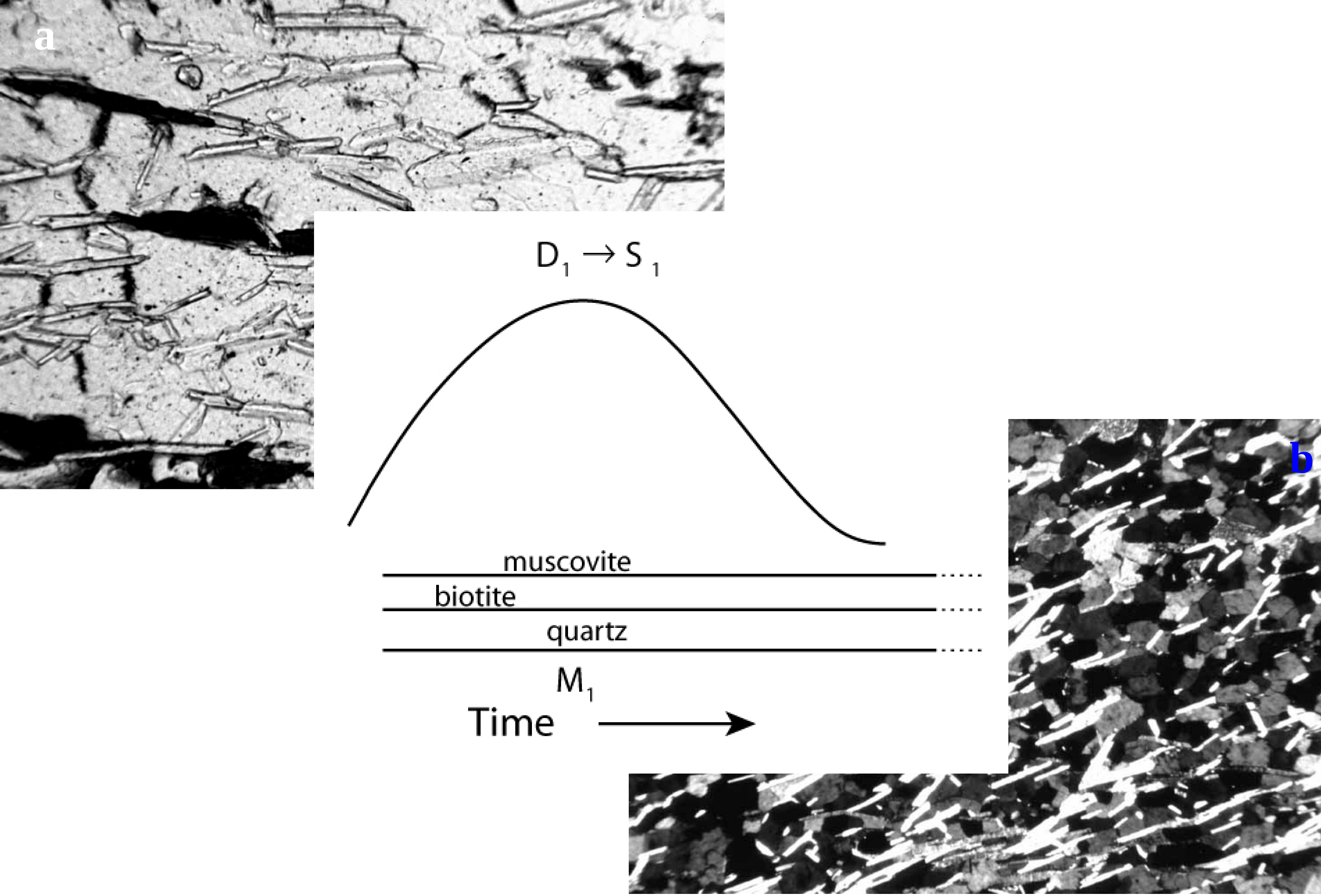

Figure 23.23. Continuous schistosity developed by dynamic recrystallization of biotite, muscovite, and quartz. a. Plane-polarized light, width of field 1 mm. b. Crossed-polars, width of field 2 mm. Although there is a definite foliation in both samples, the minerals are entirely strain-free.

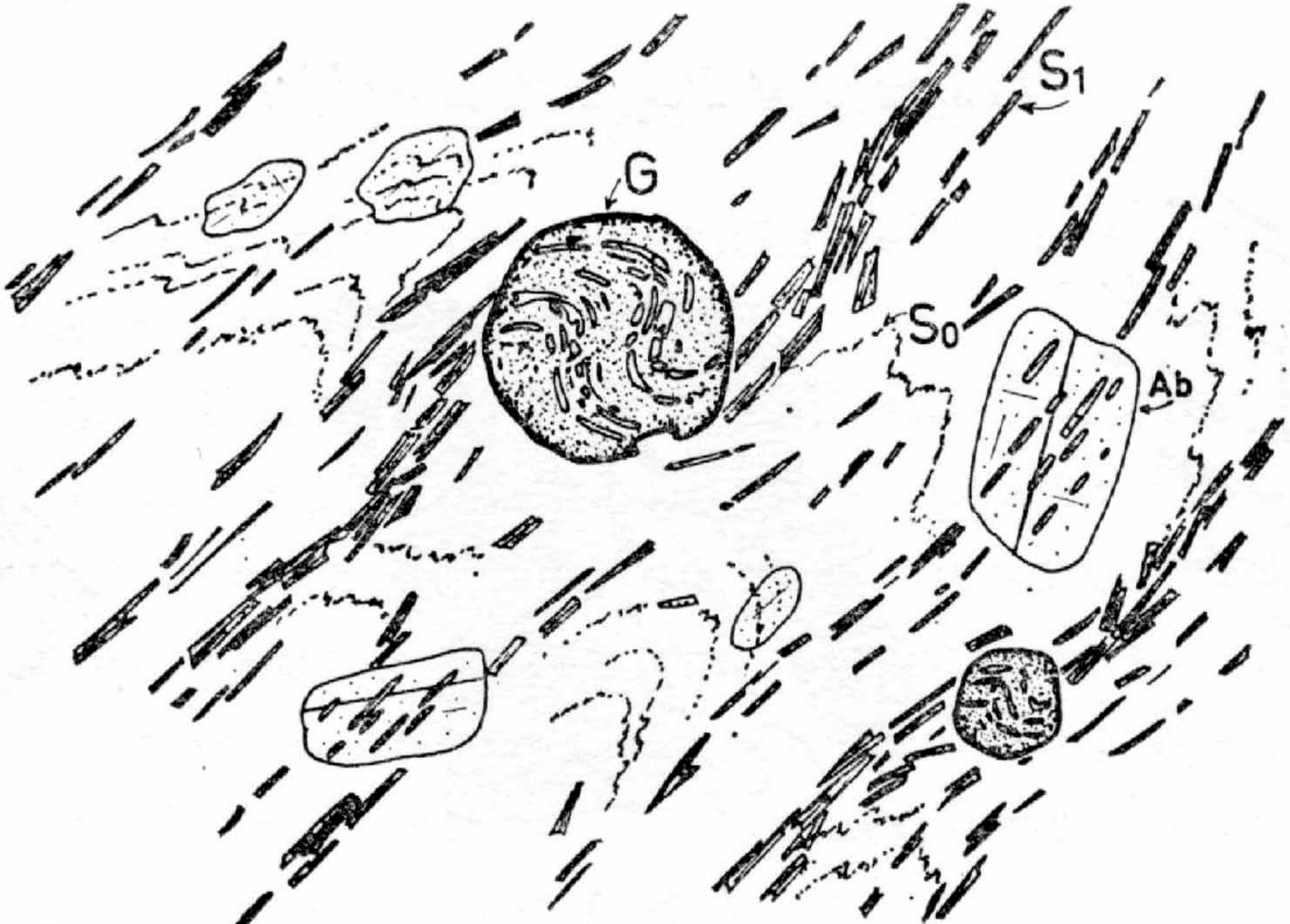

Figure 23.48a. Interpreted sequential development of a polymetamorphic rock. From Spry (1969) *Metamorphic Textures*. Pergamon. Oxford.

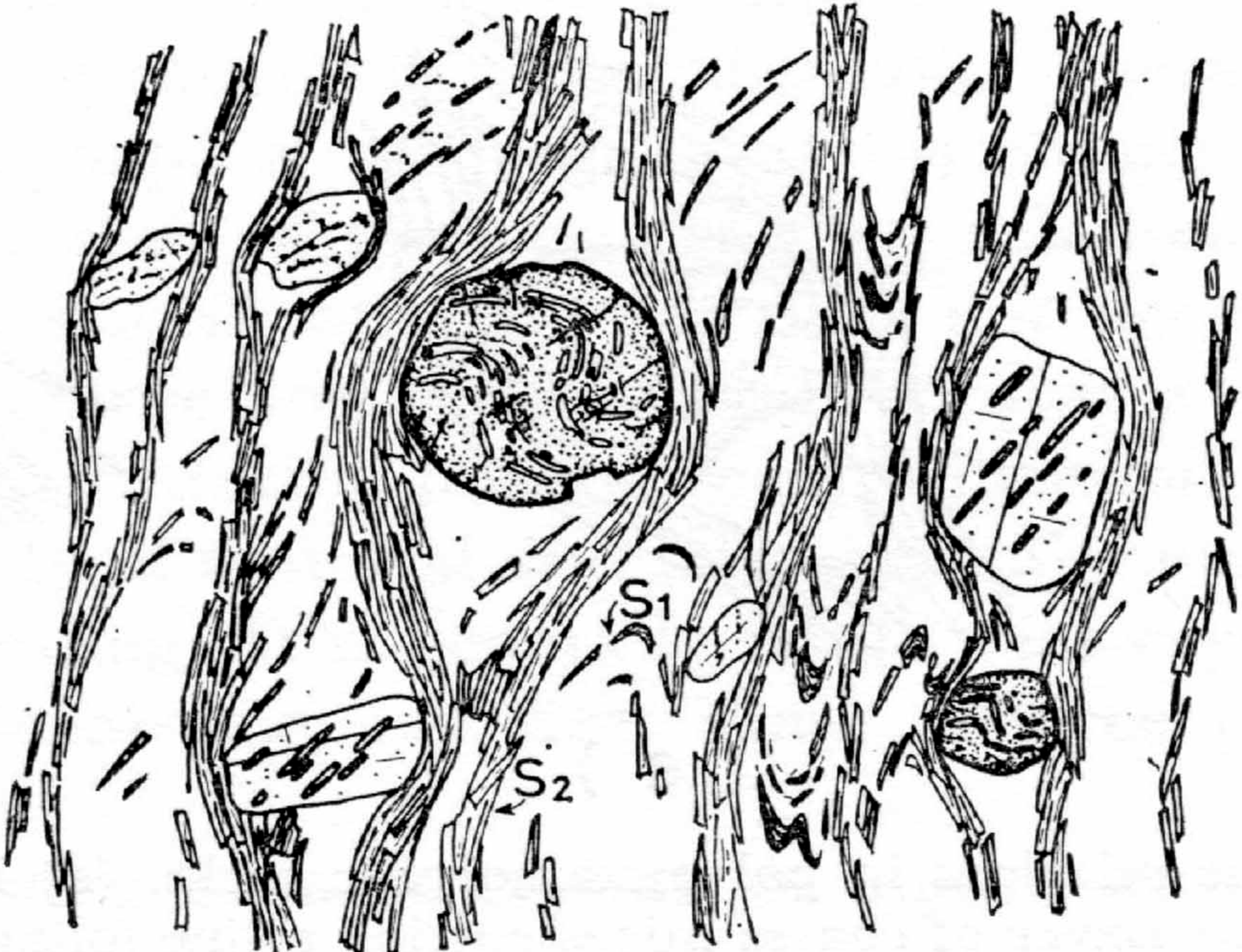

Figure 23.48b. **Interpreted sequential development of a polymetamorphic rock. From Spry (1969)** ***Metamorphic Textures*****. Pergamon. Oxford.**

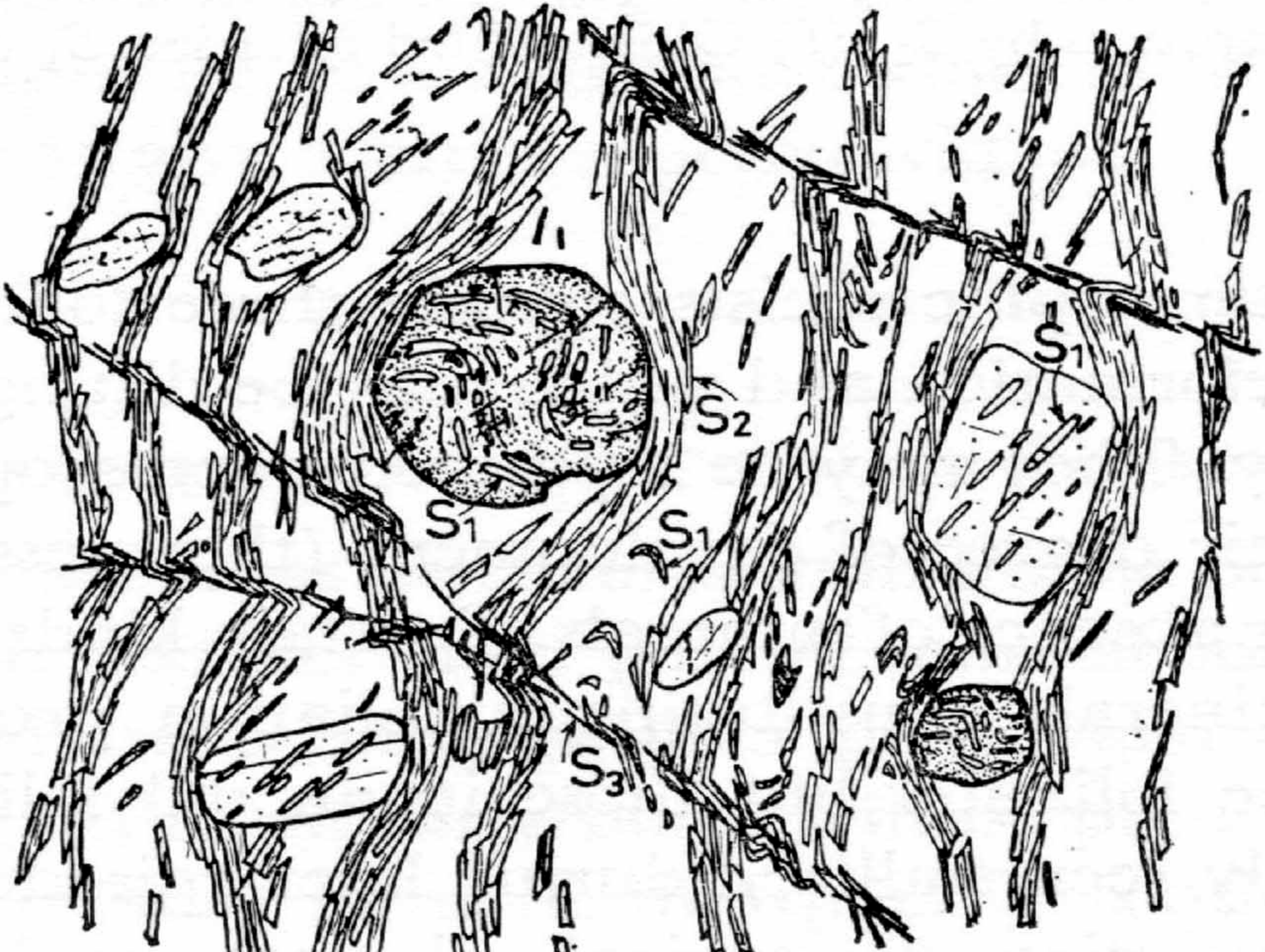

Figure 23.48c. **Interpreted sequential development of a polymetamorphic rock. From Spry (1969) *Metamorphic Textures*. Pergamon. Oxford.**

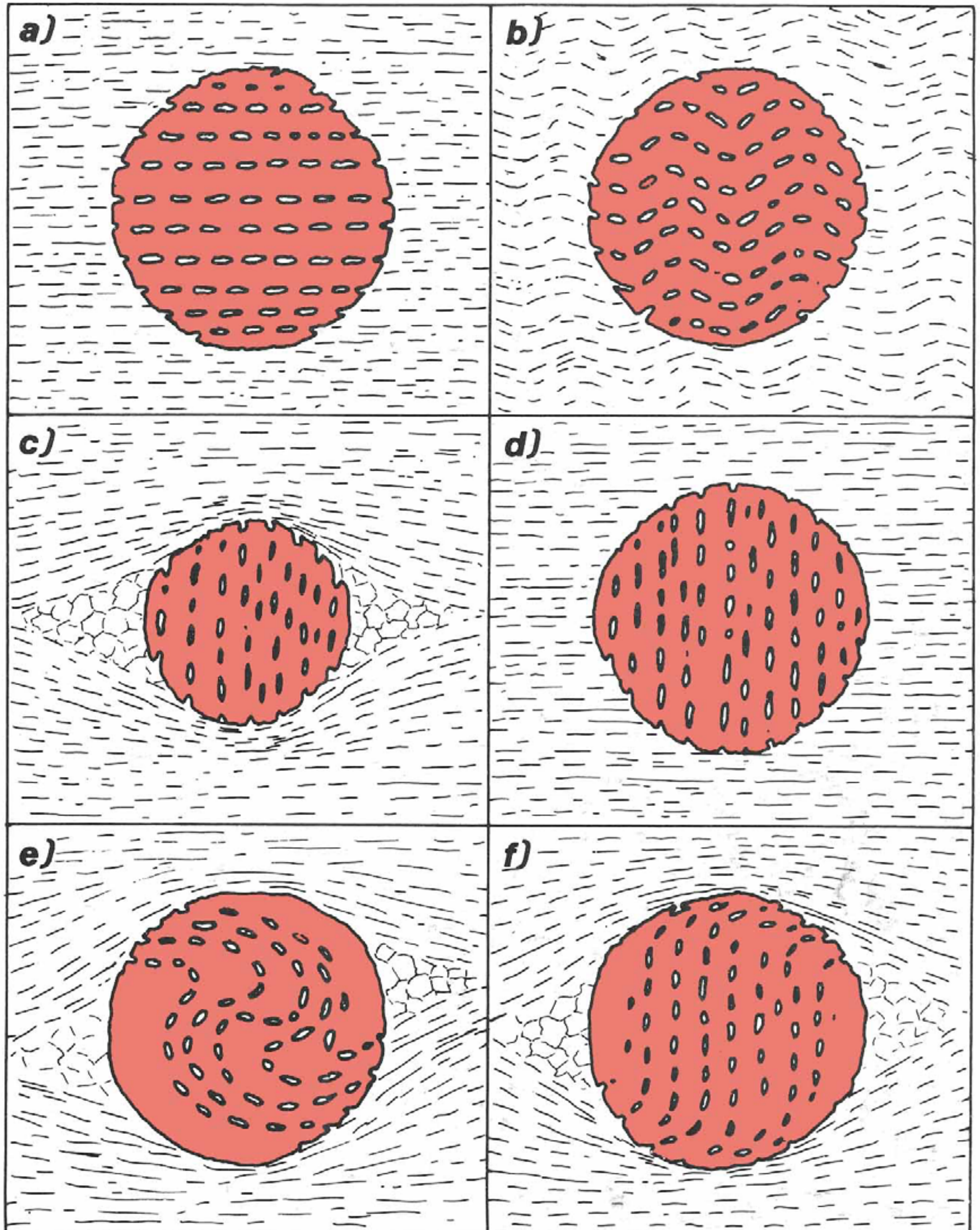

Post-kinematic: S_i is identical to and continuous with S_e

Pre-kinematic: Porphyroblasts are post-S_2. S_i is inherited from an earlier deformation. S_e is compressed about the porphyroblast in (c) and a pressure shadow develops.

Syn-kinematic: Rotational porphyroblasts in which S_i is continuous with S_e suggesting that deformation did not outlast porphyroblast growth.

From Yardley (1989) An Introduction to Metamorphic Petrology. Longman.

Deformation may not be of the same style or even coeval throughout an orogen

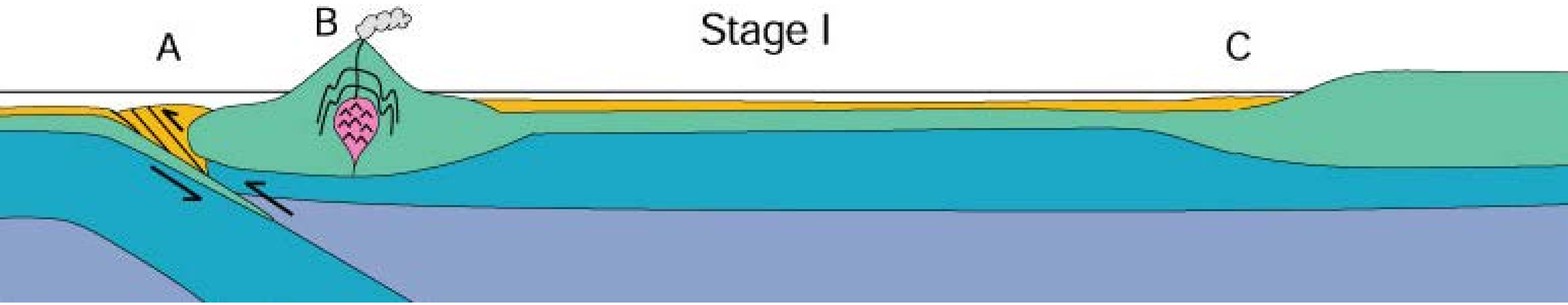

Stage I: D_1 in forearc (A) migrates away from the arc over time. Area (B) may have some deformation associated with pluton emplacement, area (C) has no deformation at all

Figure 23.49. Hypothetical development of an orogenic belt involving development and eventual accretion of a volcanic island arc terrane. After Passchier and Trouw (1996) Microtectonics. Springer-Verlag.

Deformation may not be of the same style or even coeval throughout an orogen

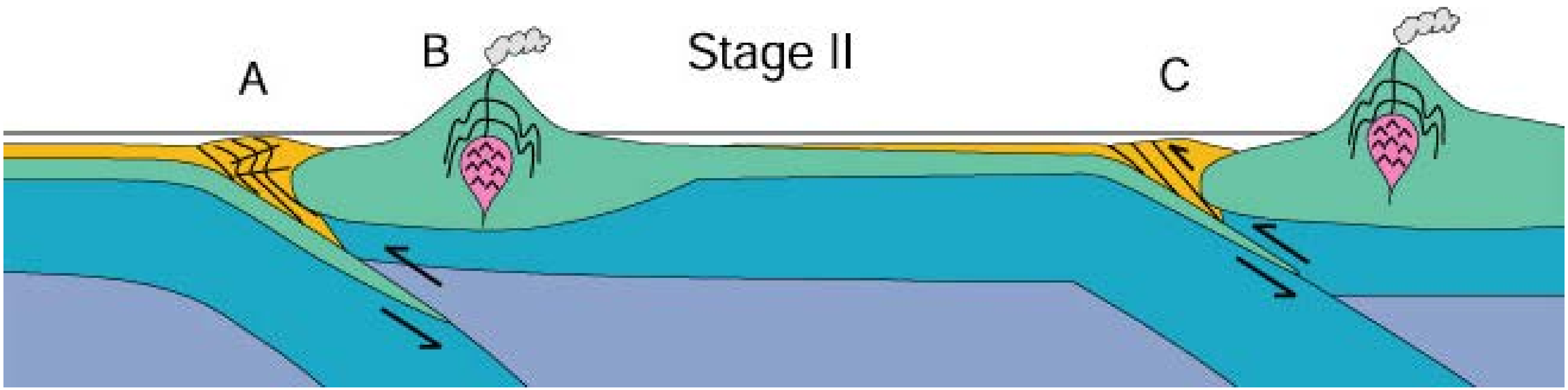

Stage II: D_2 overprints D_1 in forearc (A) in the form of sub-horizontal folding and back-thrusting as pushed against arc crust. Area (C) begins new subduction zone with thrusting and folding migrating toward trench.

Figure 23.49. Hypothetical development of an orogenic belt involving development and eventual accretion of a volcanic island arc terrane. After Passchier and Trouw (1996) Microtectonics. Springer-Verlag.

Deformation may not be of the same style or even coeval throughout an orogen

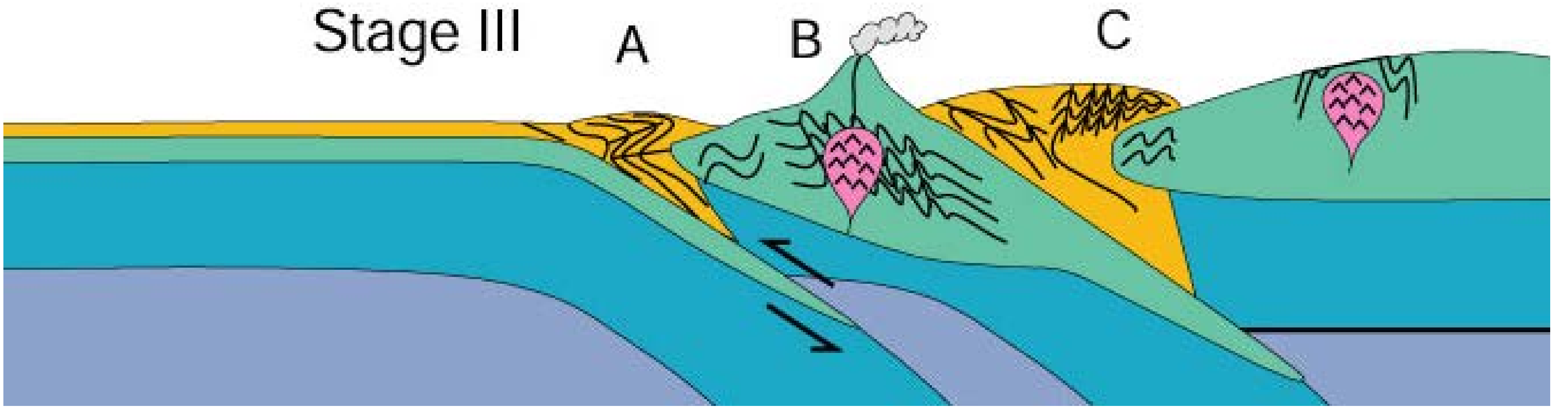

Stage III: Accretion deforms whole package. More resistant arc crust gets a D_1 event. D_2 overprints D_1 in forearc (A) and in pluton-emplacement structures in (B). Area (C) in the suture zone gets D_3 overprinting D_2 recumbent folds on D_1 foliations.

Figure 23.49. Hypothetical development of an orogenic belt involving development and eventual accretion of a volcanic island arc terrane. After Passchier and Trouw (1996) Microtectonics. Springer-Verlag.

Deformation may not be of the same style or even coeval throughout an orogen

The orogen as it may now appear following uplift and erosion.

Figure 23.49. Hypothetical development of an orogenic belt involving development and eventual accretion of a volcanic island arc terrane. After Passchier and Trouw (1996) Microtectonics. Springer-Verlag.

Replacement Textures and Reaction Rims

- Typically develop when reactions do not run to completion
- Replacement occurs when the reaction products replace a reacting mineral
- **Pseudomorph** may develop, in which the reaction products retain the shape of the original mineral
- **Symplectite** – reaction that produces intimate, typically *wormy-looking intergrowth* of two or more minerals

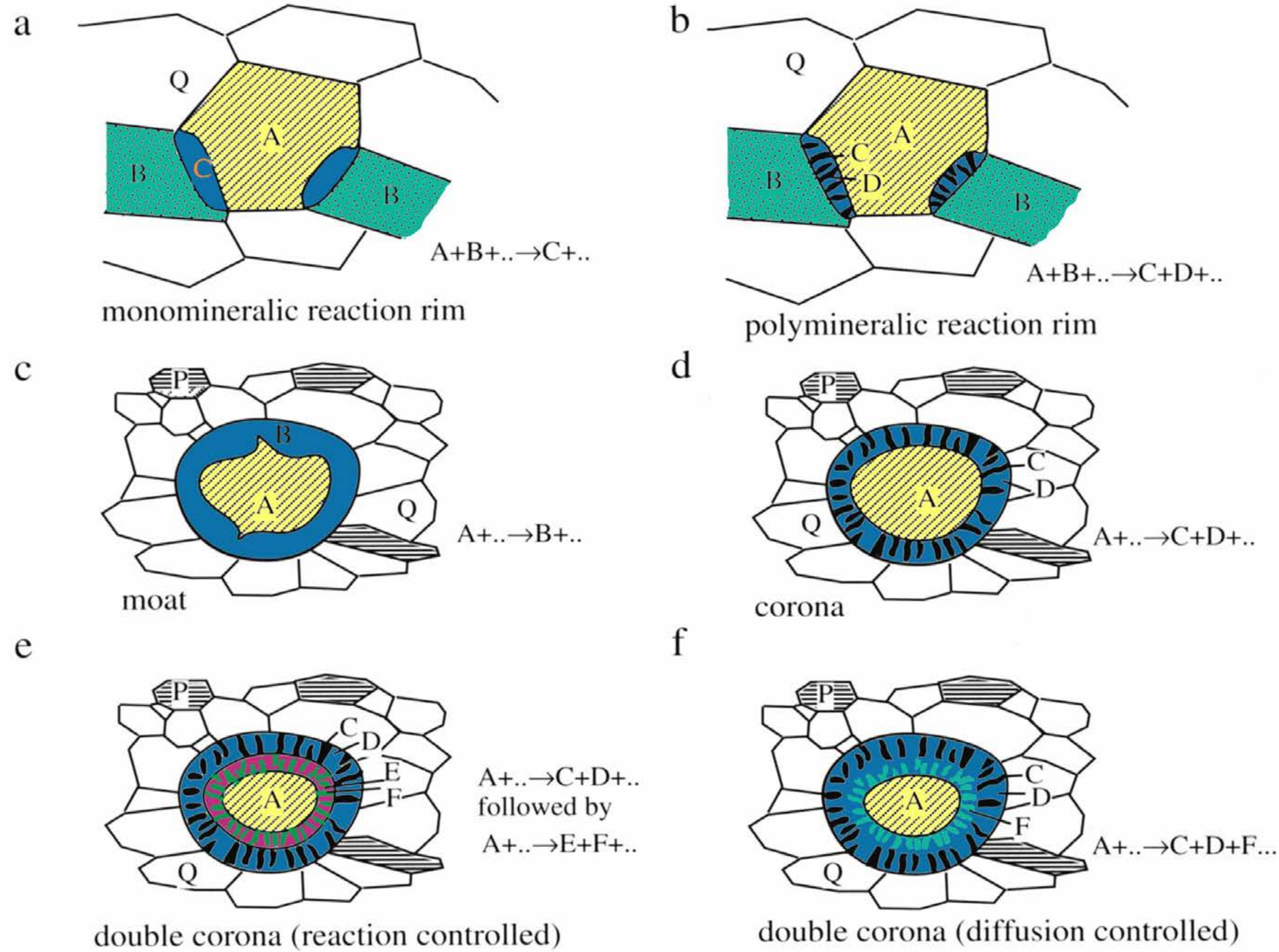

Figure 23.53. Reaction rims and coronas. From Passchier and Trouw (1996) Microtectonics. Springer-Verlag.

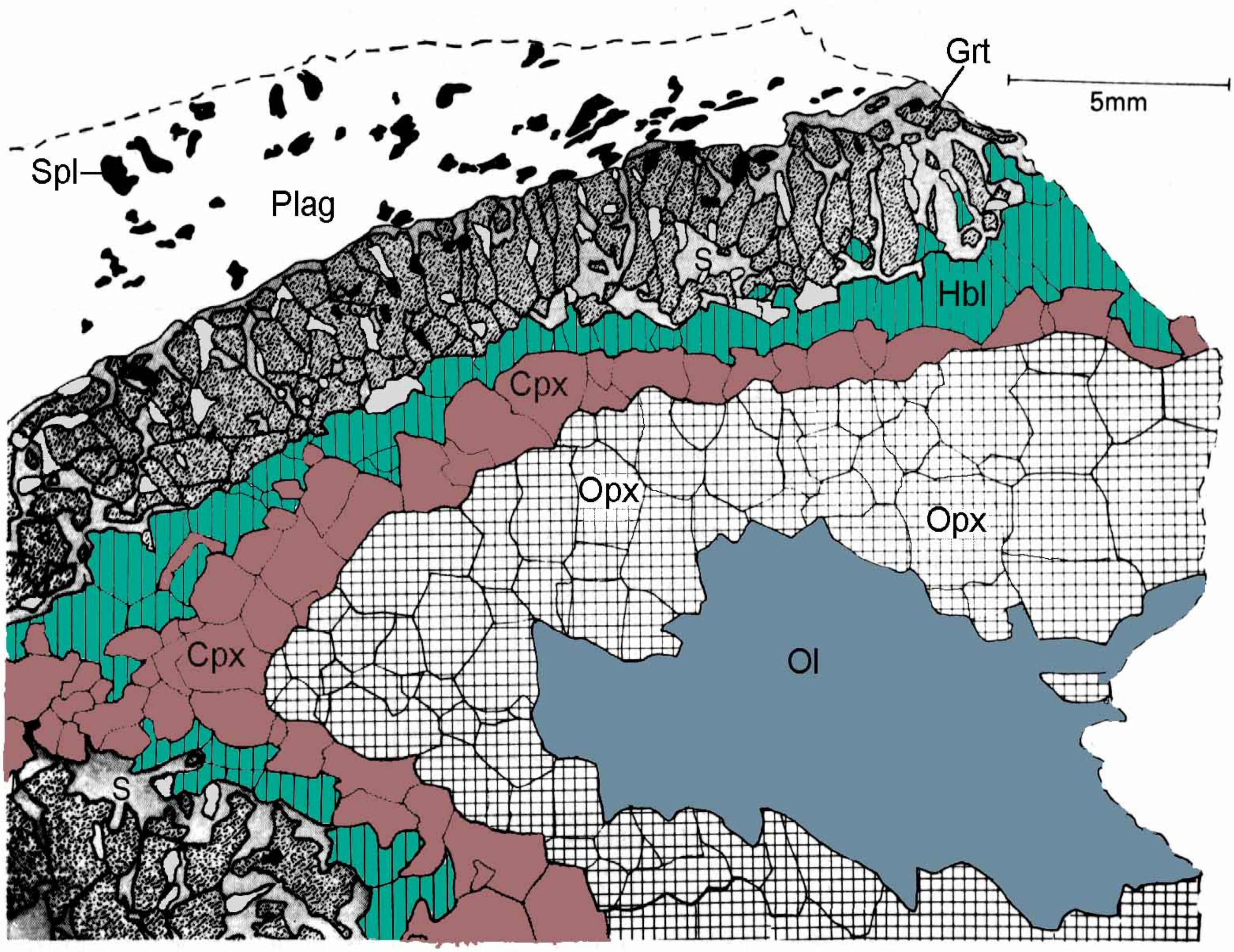

Figure 23.54. Portion of a multiple coronite developed as concentric rims due to reaction at what was initially the contact between an olivine megacryst and surrounding plagioclase in anorthosites of the upper Jotun Nappe, W. Norway. From Griffen (1971) *J. Petrol.*, 12, 219-243.

Photomicrograph of multiple reaction rims between olivine (green, left) and plagioclase (right).

Coronites in outcrop. Cores of orthopyroxene (brown) with successive rims of clinopyroxene (dark green) and garnet (red) in an anorthositic matrix. Austrheim, Norway.

Textural Geochronology

Application of radiometric dating techniques for minute samples in textural context

Determine ages of mineral growth and separate deformational/metamorphic events.

Thermal ionization mass spectrometry (TIMS): ionization of (sub-nanogram) samples on a filament and mass spectrometry of the ionized isotopes. Tiny drill can "*microsample*" pieces of single mineral grains a few tens of mm across for analysis. Mineral samples can thus be observed in thin section and microsampled from specific textural situations.

Laser-ablation inductively-coupled plasma mass spectrometry (LA-ICPMS). A high-power laser ablates a sample *in situ* and particles are fed into a mass spectrometer. Ultraviolet **(UV)** laser ablation has a spatial resolution ≤ 20 µm, so it can determine ages within zoned minerals and inclusions in porphyroblasts as they are observed microscopically.

Ion microprobe (IMP, SHRIMP), also called **secondary-ion mass spectrometry (SIMS).** Uses an ion beam (typically Cs or O) to sputter ions from a sample surface while observed in thin section and feed them into a mass spectrometer. Resolutions down to 10 µm are possible.

Electron microprobe (EMP) Some new probes are now optimized for trace element analysis and geochronology.

Textural Geochronology

Examples

Christensen et al. (1989) used TIMS to measure $^{87}Sr/^{86}Sr$ in single garnets from SE Vermont.

^{87}Rb in K-rich matrix minerals (such as biotite) → ^{87}Sr, which was then incorporated into growing garnet (which accepts Ca, hence Sr, but not Rb).

Garnets grew during the Acadian orogeny (~380 Ma).

Determined core and rim ages for three garnets → average duration of garnet growth to be 10.5±4.2 Ma. Then, by measuring garnet radii, they calculated the average growth rate: 1.4 mm/Ma. One garnet with spiral inclusions also yielded a rotational shear strain rate of 7.6×10^{-7} a^{-1} (0.76 per Ma).

Textural Geochronology

Examples

Simpson et al. (2000) TIMS isotopic ratios on monazite separates, Everest region of Nepal.

Older euhedral monazite oriented sillimanite inclusions parallel to S_1 in the matrix: growth either syn- or post-sillimanite and post S_1 (32.2±0.4 Ma).

Later lower-pressure metamorphism → cordierite and irregular-shaped monazite (yielded 22.7±0.2 Ma).

The Everest granite dated at 21.3-20.5 Ma.

Place far better constraints than earlier traditional works on post-collision metamorphism, with early Barrovian metamorphism peaking at 32 Ma and a second low-P event at 22.7 Ma (post-orogenic collapse?). Granites (probably related to collapse) emplaced at 20-21 Ma.

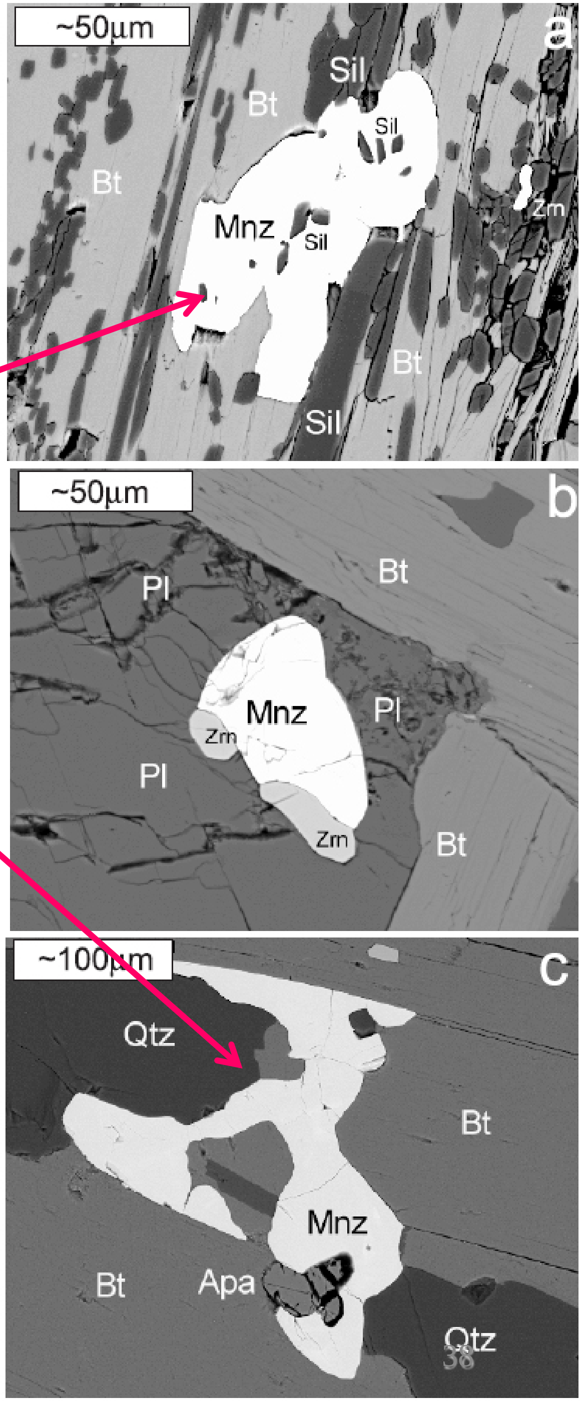

Figure 23.55 Backscattered SEM images of textural relationships of monazites from the Everest region of Nepal. **a.** Well-developed M_1 monazite enveloping sillimanite inclusions aligned sub-parallel to external S_1 foliation. **b.** Nearly euhedral M_1 monazite in the same sample surrounded by armoring plagioclase. **c.** Irregularly shaped M_2 monazite in a nearby sample. From Simpson et al. (2000).

Textural Geochronology

Examples

Müller et al. (2000) microsampled carbonate and quartz-chlorite from incrementally-developed strain fringes of σ-type mantles on pyrite porphyroclasts from a shear zone in northern Pyrenees.

Fringes developed during two distinct phases of shear (D_2 and D_3) following an earlier period of crustal shortening (D_1 - which created a foliation preserved as straight inclusion trails within the pyrites).

Pyrites thus grew as post-D_1 porphyroblasts, but were deformed during D_2 and D_3.

Notice that successive increments develop between the porphyroclast and receding earlier fringe, not at the ends of the fringe tails.

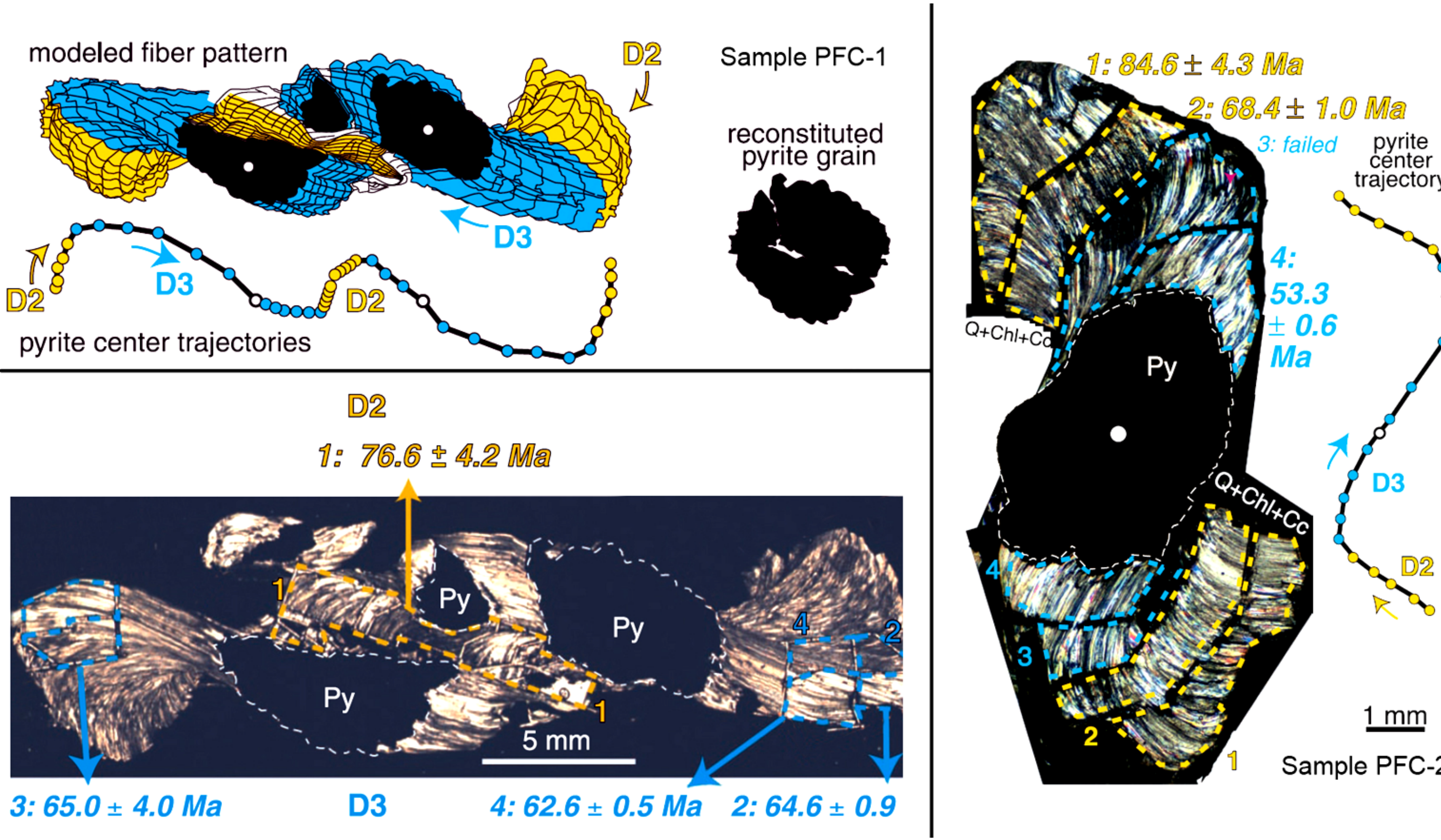

Figure 23.56 a. Broken pyrite porphyroblast with sigmoidal fibrous carbonate-quartz-chlorite strain fringe and kinematic reconstruction above. Area generated during D_2 and D_3 events are outlined with dashed lines in photomicrograph (arrows indicate Rb-Sr ages) and shaded in the reconstruction (with arrows indicating the direction of fiber growth). **b.** Photomicrograph of an unbroken pyrite porphyroblast and strain fringe with outlined growth zones and Rb-Sr ages. After Müller et al. (2000).

Figure 23.57. Ages vs. strain (ε as a percent) show a relatively slow D_2 period (strain rate ~3.5×10^{-8} a^{-1}) lasting from ~ 87 to 66 Ma, followed by a period of increasing D_3 strain rate (~2.4×10^{-7} a^{-1}) for about 4 Ma, correlated with an abrupt change in fiber growth direction (and interpreted as a stress field transformation from D_2 gravitational collapse to renewed D_3 crustal shortening). Compressive strain then wanes to earlier D_2 rates until ~50 Ma ago.

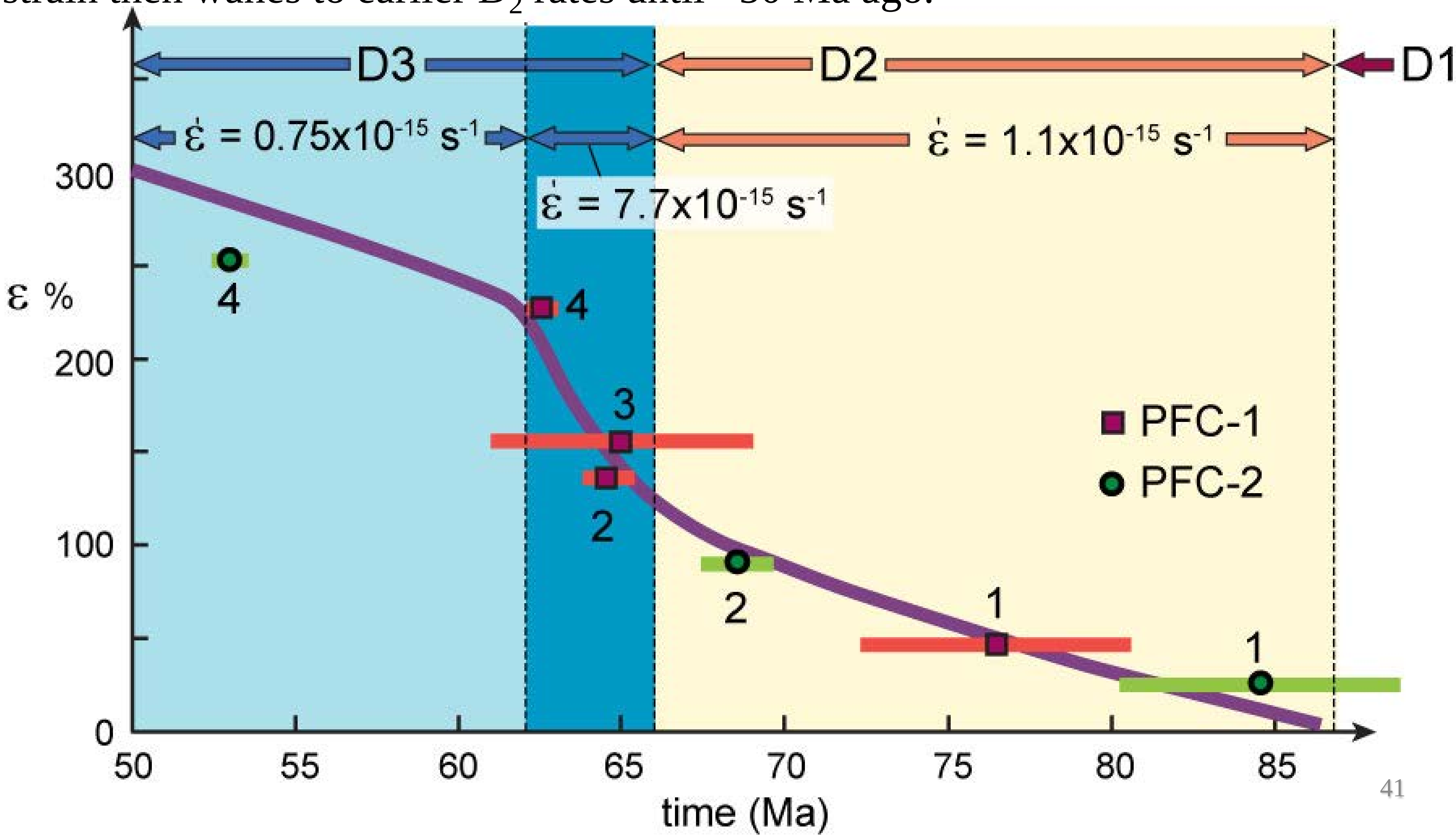

Textural Geochronology

Monazite U-Th-Pb dating

…using the electron microprobe (no mass spectrometer necessary)

Monazite is a REE-phosphate mineral

Development in metamorphic rocks is typically associated with garnet breakdown.

Monazite picks up U and Th, but virtually zero Pb, so any Pb detected is derived over time from U or Th decay.

We can thus use (U or Th)/Pb from *chemical* analysis (EMP) to yield an age. Enables many labs with EM facilities but no mass spectrometer to work.

Technique assumes 1) that all Pb in monazite is radiogenic, and 2) that the parental U isotopes occur in average crustal proportions.

Best if sufficient Pb has accumulated (i.e. early Paleozoic and older monazites).

Blocking temperatures for diffusion in monazite are in excess of 800°C, so monazite can be used to date high-grade metamorphic and even igneous events.

Textural Geochronology

Examples

Pyle and Spear (2003) and Pyle et al. (2005): four generations of monazite in migmatites from the Chesham Pond Nappe of SW New Hampshire (USA).

The first generation occurs as high-yttrium cores in zoned monazites (bright in Figure 23.58). *In situ* EMP U-Th-Pb dating yielded an age of 410±10 Ma for domain 1 cores. Pyle and co-workers speculated that these cores represent inherited pre-metamorphic monazites.

Domain 2 monazite occurs as rims on domain 1 cores and as inclusions associated with xenotime in garnet and yield an age of 381±8 Ma.

Domain 3 monazite (372±6 Ma) grew in the absence of xenotime and is thus is low in yttrium (dark in Figure 23–58).

Domain 4 monazite (352±14 Ma) occurs as thin discontinuous rims on earlier monazite and has very high Y content.

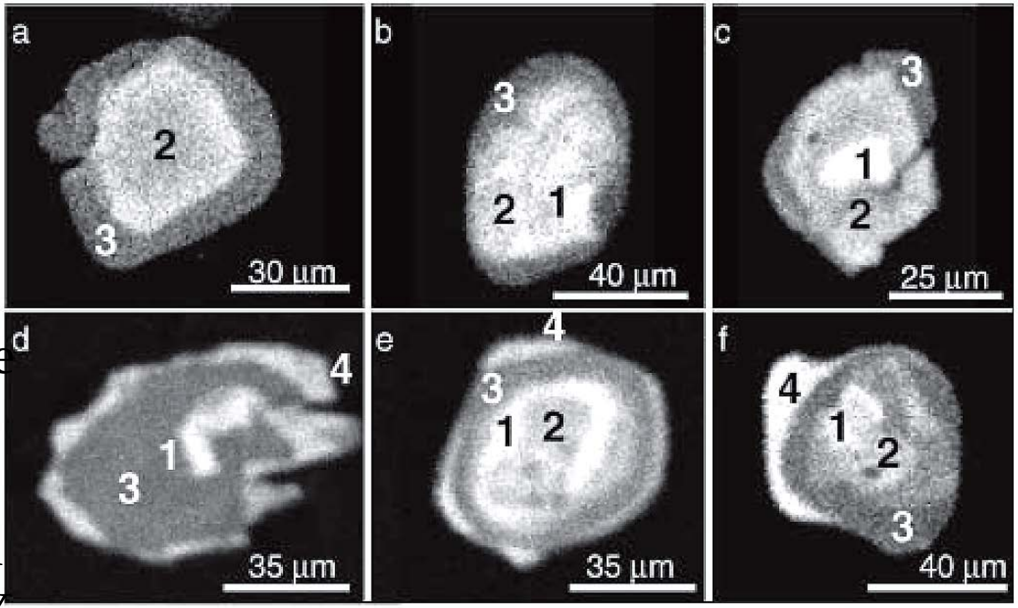

Figure 23.58 Yttrium (Y) distribution maps of zoned monazite crystals from the Chesham Pond Nappe, SW New Hampshire determined by electron microprobe (EMP) analysis. Brighter areas are higher in Y. From Pyle and Spear (2003).

Textural Geochronology

Examples

Ability to distinguish texturally separate growth stages of accessory minerals and determine ages of mm-scale domains from EMP analysis is a valuable new tool.

Relating those stages and domains to specific events and/or mineral reactions during prograde or retrograde metamorphism is an important step in relating these observations to the petrogenetic history of the rocks and area.

Pyle and Spear (2003) used the reactions and geothermobarometry to estimate the temperatures and pressures of the dated stages of petrogenesis.

They concluded that stages 2, 3, and 4 occurred along a nearly isobaric prograde path of metamorphism at about 0.3 GPa from ~ 500^{o}C to melting just over 700^{o}C.

Pyle et al. (2005) related pre-metamorphic (domain 1) monazites to the local New Hampshire Granite Series of Acadian age (~390-410 Ma).

Domains 2-4 regional metamorphism were attributed to a later heating event, ascribed to lithospheric mantle delamination and related asthenospheric upwelling.

Cooling to crystallize domain 4 monazite probably associated with overthrusting of the Chesham Pond Nappe, constrained to have begun roughly 355 Ma ago.

Textual Geochronology

Examples

Mahan et al. (2006) used EMP-based geochronology to date five events in high-P-T Precambrian granulites associated with the ductile Legs Lake shear zone in the Lake Athabasca region of the Canadian Shield.

Monazite events 1 (2570±11 Ma) and 2 (2544 to 2486 Ma) are high-Y and occur as inclusions in garnet. Appear to have grown during high-P-T granulite facies metamorphism prior to or coeval with garnet growth.

Monazite 3 is lower in yttrium (suggesting garnet was present and sequestered much) and occurs principally in the matrix or in garnet cracks. A wide range of ages (2529 to 2160 Ma) are derived from event 3 monazites suggesting episodic growth with unclear significance.

Event 4 monazite (1937-1884 Ma) interpreted as developed during a second high-P-T granulite metamorphic event. Also low in Y and coexists with garnet.

Monazites of event 5 (~1850 Ma) correlated with garnet breakdown (hence high-Y) to produce lower T and P retrograde biotite and cordierite (+ monazite). Mahan et al. (2006) related this uplift and hydration event to thrusting along the Legs Lake shear zone. Hydration, they speculated, was aided by loading and dehydration of the footwall metasediments with fluid channeled up the shear zone.

Textural Geochronology

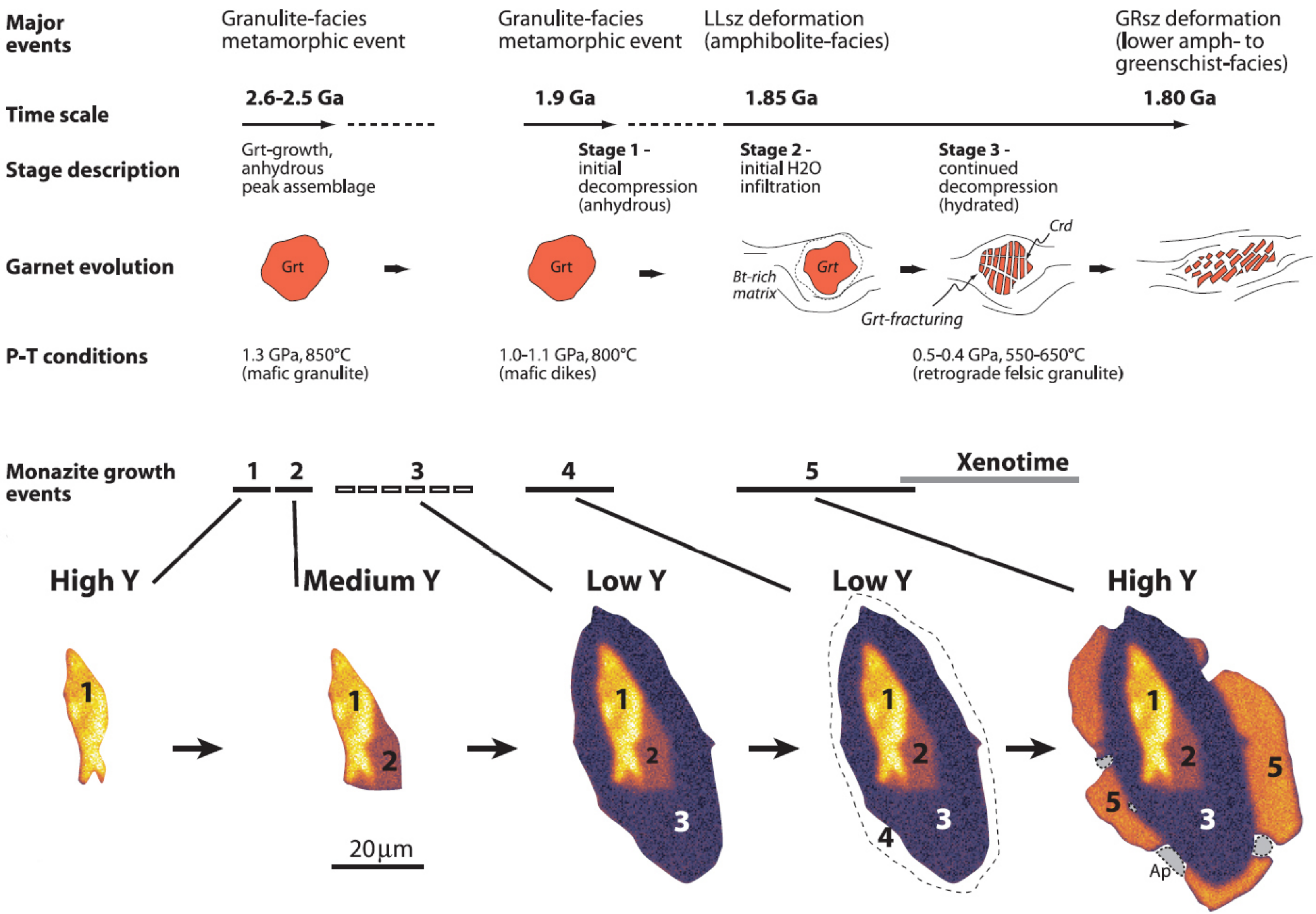

Figure 23.59 Summary model for the evolution of felsic granulites in retrograde shear zones, Snowbird Tectonic Zone, Saskatchewan, Canada. Bottom images are yttrium element maps of a zoned monazite crystal from which age determinations for the events have been derived (brighter areas are higher in Y). Possible intermediate periods of resorption are not shown. LLsz = Legs Lake shear zone. After Mahan et al. (2006).